

Indicators of Global Climate Change 2022: Annual update of large-scale indicators of the state of the climate system and the human influence

Piers M. Forster¹, Christopher J. Smith^{1,2}, Tristram Walsh³, William F. Lamb^{4,1}, Robin Lamboll⁵, Mathias Hauser⁶, Aurélien Ribes⁷, Debbie Rosen¹, Nathan Gillett⁸, Matthew D. Palmer^{9,10}, Joeri Rogelj⁵, Karina von Schuckmann¹¹, Sonia I. Seneviratne⁶, Blair Trewin¹², Xuebin Zhang⁸, Myles Allen³, Robbie Andrew¹³, Arlene Birt¹⁴, Alex Borger¹⁵, Tim Boyer¹⁶, Jiddu A. Broersma¹⁵, Lijing Cheng¹⁷, Frank Dentener¹⁸, Pierre Friedlingstein^{19,20}, José M. Gutiérrez²¹, Johannes Gütschow²², Bradley Hall²³, Masayoshi Ishii²⁴, Stuart Jenkins³, Xin Lan^{22,40}, June-Yi Lee²⁵, Colin Morice⁹, Christopher Kadow²⁶, John Kennedy²⁷, Rachel Killick⁹, Jan C. Minx^{4,1}, Vaishali Naik²⁸, Glen P. Peters¹³, Anna Pirani²⁹, Julia Pongratz^{30,39}, Carl-Friedrich Schleussner³¹, Sophie Szopa³², Peter Thorne³³, Robert Rohde³⁴, Maisa Rojas Corradi³⁵, Dominik Schumacher⁶, Russell Vose³⁶, Kirsten Zickfeld³⁷, Valerie Masson-Delmotte³², Panmao Zhai³⁸

¹Priestley Centre, University of Leeds, Leeds, LS2 9JT, UK

15 ²International Institute for Applied Systems Analysis (IIASA), Austria

³Environmental Change Institute, University of Oxford, UK

⁴Mercator Research Institute on Global Commons and Climate Change (MCC), Berlin, Germany

⁵Centre for Environmental Policy, Imperial College London, UK

20 ⁶Institute for Atmospheric and Climate Science, Department of Environmental Systems Science, ETH Zurich, Zurich, Switzerland

⁷Université de Toulouse, Météo France, CNRS, France

⁸Environment and Climate Change Canada, Canada

⁹Met Office Hadley Centre, Exeter, UK

¹⁰School of Earth Sciences, University of Bristol, UK

25 ¹¹Mercator Ocean international, Toulouse, France

¹²Bureau of Meteorology, Melbourne, Australia

¹³CICERO Center for International Climate Research, Oslo, Norway

¹⁴Backgroundstories.com, Minneapolis College of Art and Design, Minneapolis, MN, USA.

¹⁵ClimateChangeTracker.org, Data for Action Foundation, Amsterdam, Netherlands

30 ¹⁶NOAA's National Centers for Environmental Information (NCEI), Silver Spring, MD, USA

¹⁷Institute of Atmospheric Physics, Chinese Academy of Sciences, Beijing, China

¹⁸European Commission, & Joint Research Centre, Institute for Environment and Sustainability, Ispra, Italy

¹⁹Faculty of Environment, Science and Economy, University of Exeter, UK

35 ²⁰Laboratoire de Météorologie Dynamique/Institut Pierre-Simon Laplace, CNRS, Ecole Normale Supérieure/Université PSL, Paris, France

²¹Instituto de Física de Cantabria (CSIC-University of Cantabria), Spain

²²Climate Resource, Australia/Germany

²³NOAA Global Monitoring Laboratory, Boulder, CO, USA

²⁴Meteorological Research Institute, Tsukuba, Japan

40 ²⁵Research Center for Climate Sciences, Pusan National University and Center for Climate Physics, Institute for Basic Science, Pusan, Republic of Korea

²⁶German Climate Computing Center, Hamburg, Germany (DKRZ)

²⁷No affiliation, Exeter, UK.

²⁸NOAA GFDL, Princeton, New Jersey, USA

45 ²⁹Université Paris-Saclay, France; CMCC, Italy; Università Cà Foscari, Italy

³⁰University of Munich, Munich, Germany

³¹Climate Analytics, Berlin, Germany and Geography Department and IRI THESys, Humboldt-Universität zu Berlin, Berlin, Germany

50 ³²Université Paris-Saclay, CNRS, CEA, UVSQ, Laboratoire des sciences du climat et de l'environnement, 91191, Gif-sur-Yvette, France

³³ICARUS Climate Research Centre, Maynooth University, Maynooth, Ireland

³⁴Berkeley Earth, Berkeley, CA, USA

³⁵University of Chile, Santiago, Chile

³⁶NOAA's National Centers for Environmental Information (NCEI), Asheville, NC, USA

55 ³⁷Simon Fraser University, Vancouver, Canada

³⁸Chinese Academy of Meteorological Sciences, Beijing, China

³⁹Max Planck Institute for Meteorology, Hamburg, Germany

⁴⁰CIRES, University of Colorado Boulder, Boulder, CO, USA

Correspondence to: Piers. M. Forster (p.m.forster@leeds.ac.uk)

60 **Abstract.** Intergovernmental Panel on Climate Change (IPCC) assessments are the trusted source of scientific evidence for climate negotiations taking place under the United Nations Framework Convention on Climate Change (UNFCCC), including the first global stocktake under the Paris Agreement that will conclude at COP28 in December 2023. Evidence-based decision making needs to be informed by up-to-date and timely information on key indicators of the state of the climate system and of the human influence on the global climate system. However, successive IPCC reports are published at intervals of 5-10 years, creating potential for an information gap between report cycles.

We follow methods as close as possible to those used in the IPCC Sixth Assessment Report (AR6) Working Group One (WGI) report. We compile monitoring datasets to produce estimates for key climate indicators related to forcing of the climate system: emissions of greenhouse gases and short-lived climate forcers, greenhouse gas concentrations, radiative forcing, surface temperature changes, the Earth's energy imbalance, warming attributed to human activities, the remaining carbon budget and estimates of global temperature extremes. The purpose of this effort, grounded in an open data, open science approach, is to make annually updated reliable global climate indicators available in the public domain (<https://doi.org/10.5281/zenodo.7969114>, Smith et al., 2023). As they are traceable to IPCC report methods, they can be trusted by all parties involved in UNFCCC negotiations and help convey wider understanding of the latest knowledge of the climate system and its direction of travel.

The indicators show that human induced warming reached 1.14 [0.9 to 1.4] °C averaged over the 2013-2022 decade and 1.26 [1.0 to 1.6] °C in 2022. Over the 2013-2022 period, human induced warming has been increasing at an unprecedented rate of

over 0.2 °C per decade. This high rate of warming is caused by a combination of greenhouse gas emissions being at an all-time high of 54 ± 5.3 GtCO₂e over the last decade, as well as reductions in the strength of aerosol cooling. Despite this, there is evidence that increases in greenhouse gas emissions have slowed, and depending on societal choices a continued series of these annual updates over the critical 2020s decade could track a change of direction for human influence on climate.

1 Introduction

Increased greenhouse gas concentrations combined with reductions in aerosol pollution have led to rapid increases in human induced effective radiative forcing, which has in turn led to atmosphere, land, cryosphere and ocean warming (Gulev et al., 2021). This in turn has led to an intensification of many weather and climate extremes, particularly more frequent and more intense hot extremes, and heavy precipitation across most regions of the world (Seneviratne et al., 2021). Given the speed of recent change, and the need for evidence-based decision-making, this Indicators of Global Climate Change (IGCC) update assembles the latest scientific understanding on the current state of the climate system, how it is evolving and the human influence to support policymakers whilst the next IPCC assessment is under preparation. This first annual update is focused on indicators related to heating of the climate system, building from greenhouse gas emissions towards estimates of human-induced warming and the remaining carbon budget. In future years, this effort could be expanded to encompass other indicators, including global precipitation changes and related extremes.

We adopt the Global Carbon Budget ethos of a community-wide inclusive effort that synthesises work from across a large and diverse global scientific community in a timely fashion (Friedlingstein et al., 2022a). Like the Global Carbon Budget, this initiative arises from the international science community to establish a knowledge base to support policy debate and action to meet the Paris Agreement temperature goal.

This update complements other international efforts under the auspices of the Global Climate Observing System (GCOS) and the World Meteorological Organization (WMO). Annual state of the climate reports are released by WMO which use much of the same data analysed here for surface temperature and energy budget trends. The Bulletin of American Meteorological Society (BAMS) releases annual State of the Climate reports covering many essential variables including temperature and greenhouse gas concentrations. However, these reports focus on statistics from the previous year and make slightly different choices over datasets and analysis compared to the IPCC (see Sect. 5). The Global Carbon Project publishes updated carbon dioxide datasets which are used directly in this report. There is no similarly structured activity that provides all the necessary datasets to update annually the assessment of human influence on global surface temperature.

110 The update is based on methodologies for key climate indicators assessed by the IPCC Sixth Assessment Report (AR6) of the physical science basis of climate change (WGI report; IPCC, 2021a) as well as Chapter 2 of the WGIII report (Dhakal et al., 2022), and is aligned with the efforts initiated in AR6 to implement FAIR principles for reproducibility and reusability (Pirani et al., 2022, Iturbide et al., 2022). IPCC reports make a much wider assessment of the science and methodologies - we do not attempt to reproduce the comprehensive nature of these IPCC assessments here.

115 The IPCC Special Report on Global Warming of 1.5°C (SR1.5), published in 2018, provided an assessment of the level of human-induced warming and cumulative emissions to date (Allen et al., 2018) and the remaining carbon budget (Rogelj et al., 2018) to support the evidence base on how the world is progressing in terms of meeting aspects of the Paris Agreement. The AR6 WGI Report, published in 2021, assessed past, current and future changes of these and other key global climate indicators, as well as undertaking an assessment of the Earth's energy budget. It also updated its approach for estimating human-induced
120 warming and global warming level. In AR6 WGI and here, reaching a level of global warming is defined as the global surface temperature change, averaged over a 20-year period, exceeding a particular level of global warming, e.g. 1.5°C global warming. Given the current rates of change and the likelihood of reaching 1.5°C of global warming in the first half of the 2030s (Lee et al., 2021; Lee et al., 2023; Riahi et al., 2022), it is important to have robust, trusted, and also timely climate indicators in the public domain to form an evidence base for effective science-based decision making.

125

When making their assessments, authors of IPCC reports assess published literature, but also apply established published analysis methods to assessed datasets, such as that produced by the latest climate model intercomparison projects (Lee et al., 2021). The authors combine and analyze both model and observational data as part of their expert assessment, making assessments of the trustworthiness and error characteristics of different datasets. It is this synthetic analysis by IPCC authors
130 that derives the estimates of key climate indicators. Wherever possible these same assessed methodological approaches are implemented here to provide the updates with variations clearly flagged and documented. The same approach, using the same datasets (updated by 2 years) and methods as employed in WGI, was used in the AR6 Synthesis Report (2023) (AR6 SYR) report to provide an updated assessment of the latest atmospheric well mixed greenhouse gas concentrations (up to 2021) and decadal average change in global surface temperature (+1.15°C [1.00°C–1.25°C] in 2013-2022 for global surface temperature).
135 However, the assessment of human-induced warming was not updated (and therefore only covers warming up to the decade 2010-2019), nor was the remaining carbon budget updated, so the related information in the AR6 SYR report remained based on data up to the end of 2019.

140 The indicators in this first annual update give important insights into the magnitude and the pace of global warming. This paper provides the basis for a dashboard of climate indicators grounded in IPCC methodologies and directly traceable to reports published as part of the AR6 cycle. We employ datasets that can be updated on a regular basis between the publication of IPCC reports. Note that there are other similar initiatives underway to update other AR6 cycle products; for example, the evolution of the WGI Interactive Atlas (Gutiérrez et al., 2021) is being developed under the Copernicus Climate Change Service (C3S) and has potential connections and synergies with this initiative that will be explored in the future.

145

Our longer-term ambition is to rigorously track both climate system change and methodological improvements between IPCC report cycles, thereby building consistency and awareness. An example of why tracking methodological change is important was the updated estimate for historic warming (the increase in global surface temperature from 1850-1900 to 1986-2005). This was 0.08 [-0.01 to 0.12] °C higher in the AR6 than in the fifth assessment report (AR5) and SR1.5. Datasets and methods of evaluating global temperature changes altered between the AR5 and AR6, leading to a small shift in the historical temperature. This was reflected in changes between AR5 and AR6, whereas SR1.5 mostly relied on methodologies from AR5 (see AR6 WGI Cross Chapter Box 2.3, Gulev et al., 2021). Annual updates provide indications of possible future methodological shifts that subsequent IPCC reports may make as science advances and can detail their impact on perceived trends.

155 The update is organised as follows: Emissions (Sect. 2) and GHG concentrations (Sect. 3) are used to develop updated estimates of effective radiative forcing (Sect. 4). Observations of global surface temperature change (Sect. 5) and Earth's energy imbalance (Sect. 6) are key global indicators of a warming world. The global surface temperature change is formally attributed to human activity in Sect. 7, which tracks human-induced warming. Section 8 updates the remaining carbon budget to policy-relevant temperature thresholds. Section 9 gives an example of global-scale indicators associated with climate extremes of maximum land surface temperatures.

160 An important purpose of the exercise is to make these indicators widely available and understood. Plans for a web dashboard are discussed in Sect. 10, code and data availability in Sect. 11 and conclusions presented in Sect. 12. Data is available at <https://doi.org/10.5281/zenodo.7969114> (Smith et al., 2023).

165 **2. Emissions**

Historic emissions from human activity were assessed in both AR6 WGI and WGIII. Chapter 5 of WGI assessed CO₂ and CH₄ emissions in the context of the carbon cycle (Canadell et al., 2021). Chapter 6 of WGI assessed emissions in the context of understanding the climate and air quality impacts of short-lived climate forcers (Szopa et al., 2021). Chapter 2 of WGIII,

published one year later (Dhakal et al., 2022), looked at the sectoral sources of emissions and gave the most up to date understanding of the current level of emissions. This section bases its methods and data on those employed in this WGIII chapter.

2.1 Methods of estimating greenhouse gas emissions changes

Like in AR6 WGIII, net GHG emissions in this paper refer to releases of GHG from anthropogenic sources minus removals by anthropogenic sinks, for those species of gases that are reported under the common reporting format of the UNFCCC. This includes CO₂ emissions from fossil fuels and industry (CO₂-FFI); net CO₂ emissions from land use, land use change and forestry (CO₂-LULUCF); CH₄; N₂O; and fluorinated gas (F-gas) emissions. CO₂-FFI mainly comprises fossil-fuel combustion emissions, as well as emissions from industrial processes such as cement production. This excludes biomass and biofuel use by industry. CO₂-LULUCF is mainly driven by deforestation, but also includes anthropogenic removals on land from afforestation and reforestation, emissions from logging and forest degradation, emissions and removals in shifting cultivation cycles, as well as emissions and removals from other land-use change and land management activities, including peat burning and drainage. The non-CO₂ GHGs - CH₄, N₂O and F-gas emissions - are linked to the fossil-fuel extraction, agriculture, industry and waste sectors.

Global regulatory conventions have led to a two-fold categorisation of F-gas emissions (also known as halogenated gases). Under UNFCCC accounting, countries record emissions of hydrofluorocarbons (HFCs), perfluorocarbons (PFCs), sulphur hexafluoride (SF₆), and nitrogen trifluoride (NF₃) - hereinafter “UNFCCC F-gases”. However, national inventories tend to exclude halons, chlorofluorocarbons (CFCs) and hydrochlorofluorocarbons (HCFCs) - hereinafter “ODS (Ozone Depleting Substances) F-gases” - as they have been initially regulated under the Montreal protocol and its amendments. In line with the WGIII assessment, ODS-F-gases and other substances, including ozone and aerosols, are not included in our GHG emissions reporting, but are included in subsequent assessments of concentrations, effective radiative forcing, human-induced warming, carbon budgets and climate impacts in line with the WGI assessment.

There are also varying conventions used to quantify CO₂-LULUCF fluxes. These include the use of bookkeeping models, dynamic global vegetation models (DVGMs), and the national inventory approach (Pongratz et al. 2021). Each differs in terms of their applied system boundaries and definitions and are not directly comparable. However, efforts to “translate” between bookkeeping estimates and national inventories using DVGMs have demonstrated a degree of consistency between the varying approaches (Friedlingstein et al., 2022a; Grassi et al., 2023).

Each category of GHG emissions included here is covered by varying primary sources and datasets. Although many datasets cover individual categories, few extend across multiple categories, and only a minority have frequent and timely update schedules. Notable datasets include the Global Carbon Budget (GCB; Friedlingstein et al., 2022b), which covers CO₂-FFI and CO₂-LULUCF; the Emissions Database for Global Atmospheric Research (EDGAR; Crippa et al., 2022) and the Potsdam Real-time Integrated Model for probabilistic Assessment of emissions Paths (PRIMAP-hist; Gütschow et al., 2016; Gütschow and Pflüger 2023), which cover CO₂-FFI, CH₄, N₂O and UNFCCC F-gases; and the Community Emissions Data system (CEDS; O'Rourke et al., 2021), which covers CO₂-FFI, CH₄, and N₂O. As detailed below not all these datasets were employed in this update.

In AR6 WGIII, total net GHG emissions were calculated as the sum of CO₂-FFI, CH₄, N₂O and UNFCCC F-gases from EDGAR, and net CO₂-LULUCF emissions from the GCB. Net CO₂-LULUCF emissions followed the GCB convention and were derived from the average of three bookkeeping models (Hansis et al., 2015; Houghton and Nassikas, 2017; Gasser et al., 2020). Version 6 of EDGAR was used (with a fast-track methodology applied for the final year of data - 2019), alongside the 2020 version of the GCB (Friedlingstein et al., 2020). CO₂-equivalent emissions were calculated using global warming potentials with a 100-year time horizon from AR6 WGI Chapter 7 (Forster et al., 2021). Uncertainty ranges were based on a comparative assessment of available data and expert judgement, corresponding to a 90% confidence interval (Minx et al., 2021): ±8% for CO₂-FFI, ±70% for CO₂-LULUCF, ±30% for CH₄ and F-gases, and ±60% for N₂O (note that the GCB assesses one standard deviation uncertainty for CO₂-FFI as ±5%, and of ±2.6 GtCO₂ for CO₂-LULUCF; Friedlingstein et al., 2022a). The total uncertainty was summed in quadrature assuming independence of estimates per species / source. Reflecting these uncertainties, AR6 WGIII reported emissions to two significant figures only. Uncertainties in GWP100 metrics were not applied (Minx et al., 2021).

This analysis tracks the same compilation of GHGs as in AR6 WGIII. We follow the same approach for estimating uncertainties and CO₂-equivalent emissions. We also use the same type of data sources but make important changes to the specific selection of data sources to further improve the quality of the data as suggested in the knowledge gap discussion of the WGIII report (Dhakal et al., 2022). Instead of using EDGAR data (which is now available as version 7), we use GCB data for CO₂-FFI, PRIMAP-hist data for CH₄ and N₂O, and atmospheric concentrations with best-estimate lifetimes for UNFCCC F-gas emissions (Hodnebrog et al., 2020). As in AR6 WGIII we use GCB for net CO₂-LULUCF emissions, taking the average of three bookkeeping models.

There are three reasons for these specific data choices. First, national greenhouse gas emissions inventories tend to use improved, higher-tier methods for estimating emissions fluxes than global inventories such as EDGAR or CEDS (Dhakal et al., 2022; Minx et al., 2021). As GCB and PRIMAP-hist integrate the most recent national inventory submissions to the UNFCCC, selecting these databases makes best use of country-level improvements in data gathering infrastructures. Second, comprehensive reporting of F-gas emissions has remained challenging in national inventories and may exclude some military applications (see Minx et al., 2021; Dhakal et al., 2022). However, F-gases are entirely anthropogenic substances, and their concentrations can be measured effectively and reliably in the atmosphere. We therefore follow the AR6 WGI approach in making use of direct atmospheric observations. Third, the choice of GCB data for CO₂-FFI means we can integrate its projection of that year's CO₂ emissions at the time of publication (i.e., for 2022). No other dataset except GCB provides projections of CO₂ emissions on this timeframe. At this point in the publication cycle (mid-year), the other chosen sources provide data points with a two-year time lag (i.e., for 2021). While these data choices inform our overall assessment of GHG emissions, we provide a comparison across datasets for each emissions category, as well as between our estimates and an estimate derived from AR6 WGIII-like databases (i.e., EDGAR for CO₂-FFI and non-CO₂ GHG emissions, GCB for CO₂-LULUCF).

2.2 Updated global greenhouse gas emissions

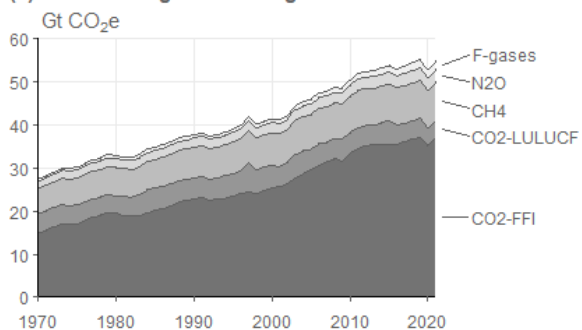
Total global GHG emissions reached 55 ± 5.2 GtCO₂e in 2021. The main contributing sources were CO₂-FFI (37 ± 3 GtCO₂), CO₂-LULUCF (3.9 ± 2.8 GtCO₂), CH₄ (8.9 ± 2.7 GtCO₂e), N₂O (2.9 ± 1.8 GtCO₂e) and F-gas emissions (2 ± 0.59 GtCO₂e). GHG emissions rebounded in 2021, following a single year decline during the COVID-19 induced lockdowns of 2020. Prior to this event in 2019, emissions were 55 ± 5.4 GtCO₂e - i.e. almost the same level as in 2021. Initial projections indicate that CO₂ emissions from fossil fuel and industry and land use change remained similar in 2022, at 37 ± 3 GtCO₂ and 3.9 ± 2.8 GtCO₂, respectively (Friedlingstein et al., 2022a). Note that ODS-F-gases such as chlorofluorocarbons and hydrochlorofluorocarbons are excluded from national GHG emissions inventories. For consistency with AR6, they are also excluded here. Including them here would increase total global GHG emissions by 1.6Gt GtCO₂e in 2021.

Average GHG emissions for the decade 2012-2021 were 54 ± 5.3 GtCO₂e. Average decadal GHG emissions have increased steadily since the 1970s across all major groups of GHG, driven primarily by increasing CO₂ emissions from fossil fuel and industry, but also rising emissions of CH₄ and N₂O. UNFCCC F-gas emissions have grown more rapidly than other greenhouse gases reported under the UNFCCC, but from low levels. By contrast, ODS F-gas emissions have declined substantially since the 1990s. Both the magnitude and trend of CO₂ emissions from land use change remain highly uncertain, with the latest data indicating an average net flux between 4-5 GtCO₂ /yr for the past few decades.

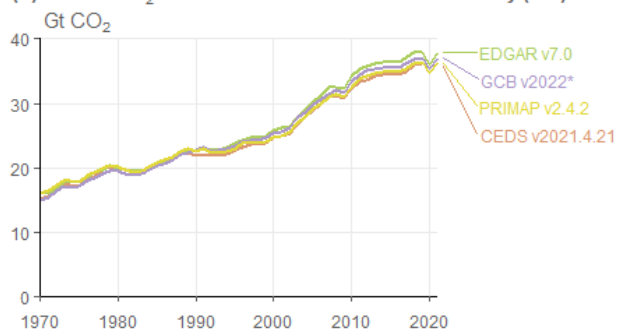
260 AR6 WGIII reported total net anthropogenic emissions of 59 ± 6.6 GtCO₂e in 2019, and decadal average emissions of 56 ± 6.0
GtCO₂e from 2010-2019. By comparison, our estimates here for the AR6 period sum to 55 ± 5.4 GtCO₂e in 2019, and 53 ± 5.3
GtCO₂e for the same decade (2010-2019). The difference between these figures, including the reduced relative uncertainty
range, is partly driven by the substantial revision in GCB CO₂-LULUCF estimates between the 2020 version (used in AR6
WGIII) of 6.6 GtCO₂ and the 2022 version (used here) of 4.6 GtCO₂. The main reason for this downward revision comes from
265 updated estimates of agricultural areas by the FAO and uses multi-annual land-cover maps from satellite remote sensing,
leading to lower emissions from cropland expansion, particularly in the tropical regions. It is important to note that this change
is not a reflection of changed and improved methodology per se, but an update of the resulting estimation due to updates in
the available input data. Second, there are relatively small changes resulting from improvements in datasets since AR6, with
the direction of changes depending on the considered gases. CH₄ accounts for the largest of these at -1.8GtCO₂e in 2019, which
270 is related to the switch from EDGAR in AR6 to PRIMAP-hist in this study. EDGAR estimates considerably higher CH₄
emissions - from fugitive fossil sources, as well as the livestock, rice cultivation and waste sectors - compared to country
reported data using higher tier methods, as compiled in PRIMAP-hist. Generally, uncertainty in these sectors is relatively high
as calculations are based on activity data and assumed emissions factors which are hard to determine and vary greatly over
countries. Differences in the remaining gases for 2019 are relatively small in magnitude (increases: N₂O (+0.18 GtCO₂e),
275 UNFCCC-F-gases (+ 0.48 GtCO₂e); and decreases: CO₂-FFI (-0.8 GtCO₂e)). Overall, excluding the change due to CO₂-
LULUCF and CH₄, they impact the total GHG emissions estimate by -0.14 GtCO₂e.

New literature not available at the time of the AR6 suggests that increases in atmospheric methane concentrations are also
driven by methane emissions from wetland changes resulting from climate change (e.g., Basu et al., 2022; Peng et al., 2022;
280 Nisbet et al., 2023; Zhang et al., 2023). Such carbon cycle feedbacks are not considered here, as we focus on estimates of
emissions resulting directly from human activities.

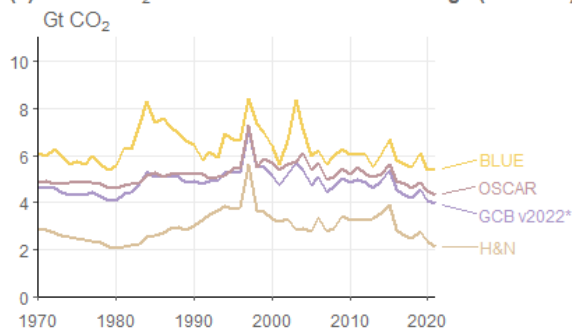
(a) Global total greenhouse gas emissions



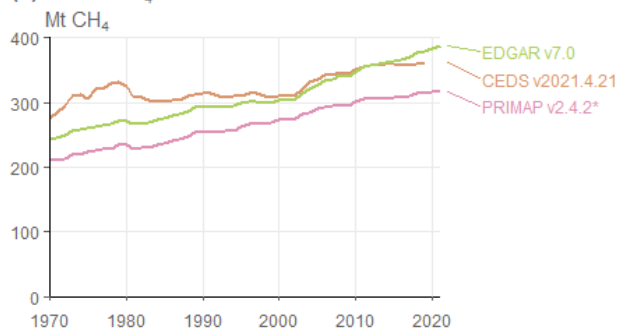
(b) Global CO₂ emissions from fossil fuel & industry (FFI)



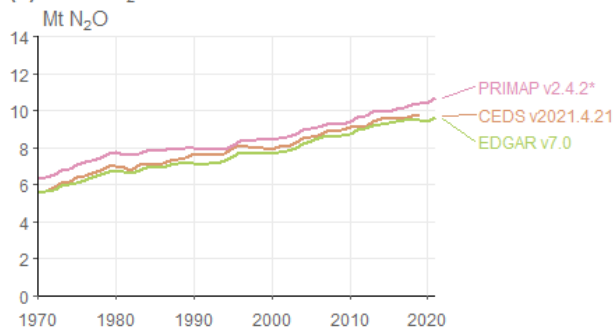
(c) Global CO₂ emissions from land use change (LULUCF)



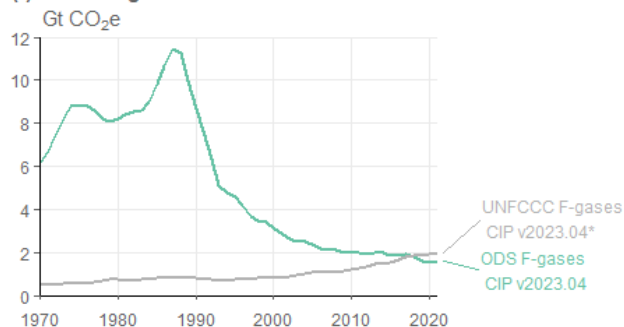
(d) Global CH₄ emissions



(e) Global N₂O emissions



(f) Global F-gas emissions



285 **Figure 1: Annual global anthropogenic greenhouse gas emissions by source, 1970-2021. Refer to Sect. 2.1 for a list of datasets. Starred datasets (*) indicate the sources used to compile global total greenhouse gas emissions in panel a. CO₂ equivalent emissions in panels a and f are calculated using GWPs with a 100-year time horizon from the AR6 WGI Chapter 7 (Forster et al., 2021). F-gas emissions in panel a) comprise only UNFCCC F-gases (see Sect. 2.1 for a list of species).**

Table 1: Global anthropogenic greenhouse gas emissions by source and decade.

Gt CO ₂ e	1970- 1979	1980- 1989	1990- 1999	2000- 2009	2010- 2019	2012- 2021	2021	2022 (projection)
GHG	30±4	35±4.4	39±4.9	45±5.1	53±5.3	54±5.3	55±5.2	
CO₂-FFI	17±1.4	20±1.6	24±1.9	29±2.3	36±2.8	36±2.9	37±3	37±3
CO₂-LULUCF	4.4±3.1	4.8±3.4	5.3±3.7	5±3.5	4.7±3.3	4.5±3.2	3.9±2.8	3.9±2.8
CH₄	6.2±1.9	6.6±2	7.3±2.2	8±2.4	8.6±2.6	8.7±2.6	8.9±2.7	
N₂O	1.9±1.1	2.1±1.3	2.2±1.3	2.4±1.5	2.7±1.6	2.8±1.7	2.9±1.8	
UNFCCC F-gases	0.58±0.17	0.78±0.23	0.77±0.23	1±0.3	1.5±0.46	1.7±0.5	2±0.59	

Notes: All numbers refer to decadal averages, except for annual estimates in 2021 and 2022. CO₂ equivalent emissions are calculated using GWP with a 100-year time horizon from AR6 WGI Chapter 7 (Forster et al., 2021). Projections of non-CO₂ GHG emissions in 2022 remain unavailable at the time of publication. Uncertainties are ±8% for CO₂-FFI, ±70% for CO₂-LULUCF, ±30% for CH₄ and F-gases, and ±60% for N₂O, corresponding to a 90% confidence interval. ODS F-gases are excluded, as noted in Sect. 2.1.

2.3 Non-methane short lived climate forcers

In addition to GHG emissions, we provide an update of anthropogenic emissions of non-methane short-lived climate forcers (SLCFs) (SO₂, BC, OC, NO_x, VOCs, CO and NH₃). HFCs are considered in Sect. 2.2. Updating emissions of many short-lived climate forcing agents to 2022 based on established datasets is not possible as compiling global data can take several years. Yet, as SLCF emissions are needed in this paper to update effective radiative forcing (ERF) estimates through 2022, updated emission datasets, where they are available, are combined with projected data to make SLCF emission time series complete.

As in Dhakal et al. (2022), sectoral emissions of SLCFs are derived from two sources. For fossil fuel, industrial, waste and agricultural sectors, we use the CEDS dataset that provided SLCF emissions for the sixth climate model intercomparison project (CMIP6) (Hoesly et al., 2018). CEDS provides global emissions totals from 1750 to 2019 in its most recent version (O'Rourke et al., 2021). No CEDS emissions data is yet available beyond 2019. As a first estimate, the SLCF emissions time series are extrapolated to 2022 using the “two-year blip” scenario (Forster et al., 2020) of global emissions suppressed by the

310 economic slowdown due to COVID-19. These projections are proxy estimates from Google and Apple mobility data over 2020, and assume a slow return to pre-pandemic emissions activity levels by 2022. Other near-real time emissions estimates covering the COVID-19 pandemic era tend to show less of an emissions reduction than the two-year blip scenario (Guevara et al., 2023). It should be stressed that accurate quantification of SLCF emissions during this period is not possible.

315 We do not explicitly account for the introduction of strict fuel sulphur controls brought in by the International Maritime Organization on 1 January 2020, which was expected to reduce SO₂ emissions from the global shipping sector by 8.5 Tg against a pre-COVID baseline (around 10% of 2019 total SO₂ emissions). SO₂ reductions from shipping are partly accounted for in the proxy activity dataset, and including a specific shipping adjustment may double-count emissions reductions.

320 For biomass burning SLCF emissions we follow AR6 WGIII (Dhakal et al., 2022) and use the Global Fire Emissions Dataset (GFED, Randerson et al., 2017) for 1997 to 2022, with the dataset extended back to 1750 for CMIP6 (van Marle et al., 2017). Estimates from 2017 to 2022 are provisional. The potential for both sources of emissions data to be updated in future versions exist, particularly in light of a forthcoming update to CEDS and quantification of shipping sector SO₂ reductions. Other natural emissions, which are important for gauging some SLCF concentrations, are considered as constant in the context of calculating concentrations and ERF.

325

Estimated emissions used here are based on a combination of GFED emissions for biomass-burning emissions and CEDS up until 2019 extended with the “two-year blip” scenario for fossil, agricultural, industrial and waste sectors. Under this scenario, emissions of all SLCFs are reduced in 2022 relative to 2019 (Table 2). As described in Sect. 4, this has implications for several categories of anthropogenic radiative forcing. Trends in SLCFs emissions are spatially heterogeneous (Szopa et al., 2021) with strong shifts in the geographical distribution of emissions over the 2010-2019 decade. Very different lockdown measures have been applied for COVID around the world resulting in various length and intensity of activity reductions and effect on air pollutant emissions (Sokhi et al., 2021). SLCF emissions have been seen to return to their pre-COVID levels by 2022 in some regions, sometimes with rebound effect, but not in all (Putaud et al., 2023, Lonsdale and Sun, 2023) but quantification at the global scale is not yet available.

335

Uncertainties associated with these emission estimates are difficult to quantify. From the non-biomass burning sectors they are estimated to be smallest for SO₂ ($\pm 14\%$), largest for black carbon (BC) (a factor of two), and intermediate for other species (Smith et al., 2011; Bond et al., 2013; Hoesly et al., 2018). Uncertainties are also likely to increase both backwards in time (Hoesly et al., 2018), and again in the most recent years. The estimates of non-biomass burning emissions for 2020, 2021 and 340 2022 are highly uncertain owing to the use of proxy activity data, scenario extension, and the impact of sulphur controls in the

shipping sector. Future updates of CEDS are expected to include uncertainties (Hoesly et al., 2018). Even though trends over recent years are uncertain, the general decline in some SLCF emissions derived is supported by aerosol optical depth measurements (e.g. Quaas et al., 2022).

345 **Table 2: Emissions of the major SLCFs in 1750, 2019 and 2022**

Compound Species	1750 emissions (Tg yr⁻¹)	2019 emissions (Tg yr⁻¹)	2022 emissions (Tg yr⁻¹)
Sulphur dioxide (SO₂) + sulphate (SO₄²⁻)	0.3	85.9	76.9
Black carbon (BC)	2.1	7.8	6.7
Organic carbon (OC)	15.4	34.7	26.0
Ammonia (NH₃)	6.6	66.5	65.3
Oxides of nitrogen (NO_x)	19.4	142.9	131.8
Volatile organic compounds (VOCs)	60.6	227.2	189.6
Carbon monoxide (CO)	348.4	937.8	764.1

Notes. Emissions of SO₂ + SO₄²⁻ use SO₂ molecular weights. Emissions of NO_x use NO₂ molecular weights. VOCs are for the total mass.

3 Well-mixed greenhouse gas concentrations

AR6 WGI assessed well mixed GHG concentrations in Chapter 2 (Gulev et al., 2021) and additionally provided a dataset of concentrations of 52 well-mixed GHGs from 1750 to 2019 in its Annex III (IPCC, 2021c). Footnotes in AR6 SYR updated
 350 CO₂, CH₄ and N₂O concentrations to 2021 (Lee et al., 2023). In this update we extended the record to 2022 for all 52 gases.

Ozone is an important greenhouse gas with strong regional variation both in the stratosphere and troposphere (Szopa et al., 2021). Its ERF arising from its regional distribution is assessed in Sect. 4 but following AR6 convention is not included with the GHGs discussed here. Other non-methane SLCFs are heterogeneously distributed in the atmosphere and are also not

355 typically reported in terms of a globally averaged concentration. Globally averaged concentrations for these are normally model derived, supplemented by local monitoring networks and satellite data (Szopa et al., 2021).

As in AR6, CO₂ concentrations are taken from the NOAA Global Monitoring Laboratory (GML) and updated through 2022 (Lan et al., 2023a). Although here CO₂ is reported on the updated WMO-CO₂-X2019 scale, whereas in AR6, values were
360 reported on the WMO-CO₂-X2007 scale. This improved calibration increases CO₂ concentrations by around 0.2 ppm (Hall et al., 2021). In AR6, CH₄ and N₂O were reported as the average from NOAA and the Advanced Global Atmospheric Gases Experiment (AGAGE) global networks. For 2022 as updated AGAGE data is not currently available, we used only NOAA data [Lan et al., 2023b], and multiplied N₂O by 1.0007 to be consistent with a NOAA-AGAGE average. NOAA CH₄ in 2022 was used without adjustment since the NOAA and AGAGE global means CH₄ are consistent within 2 ppb. Mixing ratio
365 uncertainties for 2022 are assumed to be similar to 2019, and we adopt the same uncertainties as assessed in AR6 WGI.

Many halogenated greenhouse gases are reported on a global mean basis from NOAA and/or AGAGE until 2020 or 2021 (SF₆ is available in the NOAA dataset up to 2022). Where both NOAA and AGAGE data are used for the same gas, we take a mean of the two datasets. Where both networks are used and the last full year of data availability is different, the difference between
370 the dataset mean and the dataset with the longer time series in this last year is used as an additive offset to the dataset with the longer time series. Some obvious inconsistencies are removed such as sudden changes in concentrations when missing data is reported as zero.

Some of the more minor halogenated gases are not part of the NOAA or AGAGE operational network and are currently only
375 reported in literature sources until 2019, or possibly 2015 (Droste et al., 2020; Laube et al., 2014; Schoenenberger et al., 2015; Simmonds et al., 2017; Vollmer et al., 2018). Concentrations of gases where 2022 data is not yet available are extrapolated forwards to 2022 using the average growth rate over the last 5 years of available data. These assumptions have an imperceptible effect on the total ERF assessed in Sect. 4, whereas excluding these gases would have an impact.

380 The global surface mean mixing ratios of CO₂, CH₄ and N₂O in 2022 were 417.1 [± 0.4] ppm, 1911.9 [± 3.3] ppb and 335.9 [± 0.4] ppb. Concentrations of all three major GHGs have increased from 2019 values reported in AR6 WGI, which were 410.1 [± 0.36] ppm for CO₂, 1866.3 [± 3.2] ppb for CH₄ and 332.1 [± 0.7] ppb for N₂O. CO₂ concentrations in 2019 are updated to 410.3 ppm using the new WMO-CO₂-X2019 scale adopted here. Concentrations of most categories of halogenated GHGs have increased from 2019 to 2022: from 109.4 to 114.2 ppt on a CF₄-equivalent scale for PFCs; 237.1 ppt to 287.2 ppt on an
385 HFC-134a-equivalent scale for HFCs; 9.9 ppt to 11.0 ppt for SF₆ and 2.1 to 2.8 ppt for NF₃. Only Montreal Protocol halogenated GHGs have decreased in concentration, from 1031.9 ppt in 2019 to 1016.6 ppt in 2022 on a CFC-12-equivalent scale,

demonstrating the continued success of the Montreal Protocol. Although even here, concentrations of some minor CFCs are rising (see also Western et al. 2023). In this update we employ AR6 derived uncertainty estimates and do not perform a new assessment. Table S3.1 in Sect. 3 of the Supplementary Material shows specific updated concentrations for all the GHGs considered.

4 Effective Radiative Forcing (ERF)

ERFs were principally assessed in Chapter 7 of AR6 WGI (Forster et al., 2021). Chapter 7 focussed on assessing ERF from changes in atmospheric concentrations, it also supported estimates of ERF in Chapter 6 that attributed forcing to specific precursor emissions (Szopa et al., 2021) and also generated the time history of ERF shown in AR6 WGI Figure 2.10 and discussed in Chapter 2 (Gulev et al., 2021). Only the concentration-based estimates are updated this year. The emission-based estimates relied on specific chemistry climate model integrations and a consistent method of applying updates to these would need to be developed in the future.

Each IPCC report has successively updated both the method of calculation and the time history of different warming and cooling contributions, measured as ERFs. Both types of updates have contributed to a significantly changed forcing estimate between successive reports. For example, Forster et al., (2021) updated the methodology to exclude land-surface temperature related adjustments from the forcing calculation, which generally increased estimates. At the same time GHG levels increased and the time history of aerosol forcing was revised, overall leading to a higher total ERF estimate in AR6 compared to AR5. These IPCC updates flow from an assessment of varied literature and also rely on updates to concentrations and/or emissions.

There is no published regularly updated total ERF indicator outside of the IPCC process, although the European Copernicus programme has trialed such a product (Bellouin et al., 2020). For radiative forcing, NOAA annually updates estimates for the main GHGs, calculating radiative forcing (RF) using the set of formulas to estimate RFs from concentrations (Montzka, 2022). Updated RF formulas were employed in AR6 (Forster et al., 2021) and these updated expressions are also employed here in Supplementary Material, Sect. 4.

The ERF calculation follows the methodology used in AR6 WGI (Smith et al., 2021). For each category of forcing, a 100,000-member probabilistic Monte Carlo ensemble is sampled to span the assessed uncertainty range in each forcing. All uncertainties are reported as 5-95% ranges and provided in square brackets. The only significant methodological change compared to AR6 is for the volcanic ERF estimate. Firstly, the preindustrial baseline data has been improved by switching to a new longer record of stratospheric aerosol optical depth before 1750 (Sigl et al, 2022). Secondly, choices have also been made to include the

January 2022 eruption of Hunga Tonga-Hunga Ha'apai as an exceptional positive ERF perturbation from the increase in stratospheric water vapour (Millan et al., 2022; Sellito et al., 2022; Jenkins et al., 2023). The methods are all detailed in Supplementary Material, Sect. 4.

420

The summary results for the anthropogenic constituents of ERF and solar irradiance in 2022 relative to 1750 are shown in Figure 2a. In Table 3 these are summarised alongside the equivalent ERFs from AR6 (1750-2019) and AR5 (1750-2011). Figure 2b shows the time evolution of ERF from 1750 to 2022.

425 Total anthropogenic ERF has increased to 2.91 [2.19 to 3.63] W m^{-2} in 2022 relative to 1750, compared to 2.72 [1.96 to 3.48] W m^{-2} for 2019 relative to 1750 in AR6. The main contributions to this increase are from increases in greenhouse gas concentrations and a reduction in the magnitude of aerosol forcing. Decadal trends in ERF have increased markedly and are now over 0.6 W m^{-2} per decade. These are discussed further in the discussion and conclusions (Sect. 12).

430 The ERF from well-mixed GHGs is 3.45 [3.14 to 3.75] W m^{-2} for 1750-2022, of which 2.25 W m^{-2} is from CO_2 , 0.56 W m^{-2} from CH_4 , 0.22 W m^{-2} from N_2O and 0.41 W m^{-2} from halogenated gases. This is an increase from 3.32 [3.03 to 3.61] W m^{-2} for 1750-2019 in AR6. ERFs from CO_2 , CH_4 and N_2O have all increased since the AR6 WG1 assessment for 1750-2019 owing to increases in atmospheric concentrations.

435 The total aerosol ERF (sum of the ERF from aerosol radiation interactions (ERFari) and aerosol cloud interactions (ERFaci)) for 1750-2022 is -0.98 [-1.58 to -0.40] W m^{-2} compared to -1.06 [-1.71 to -0.41] W m^{-2} assessed for 1750-2019 in AR6 WG1. This continues a trend of weakening aerosol forcing due to reductions in precursor emissions. Most of this reduction is from ERFaci which is determined to be -0.77 [-1.33 to -0.23] W m^{-2} compared to -0.84 [-1.45 to -0.25] W m^{-2} in AR6 for 1750-2019. ERFari for 1750-2022 is -0.21 [-0.42 to 0.00] W m^{-2} , marginally weaker than the -0.22 [-0.47 to 0.04] W m^{-2} assessed for 1750-
440 2019 in AR6 WG1 (Forster et al., 2021). The largest contributions to ERFari are from SO_2 (primary source of sulphate aerosol; -0.21 W m^{-2}), BC (+0.12 W m^{-2}), OC (-0.04 W m^{-2}) and NH_3 (primary source of nitrate aerosol; -0.03 W m^{-2}). ERFari is not weakening as fast as ERFaci due to reductions in the warming influence of BC cancelling out some of the reduced sulphate cooling. ERFari also includes terms from CH_4 , N_2O and NH_3 which are small but have all increased.

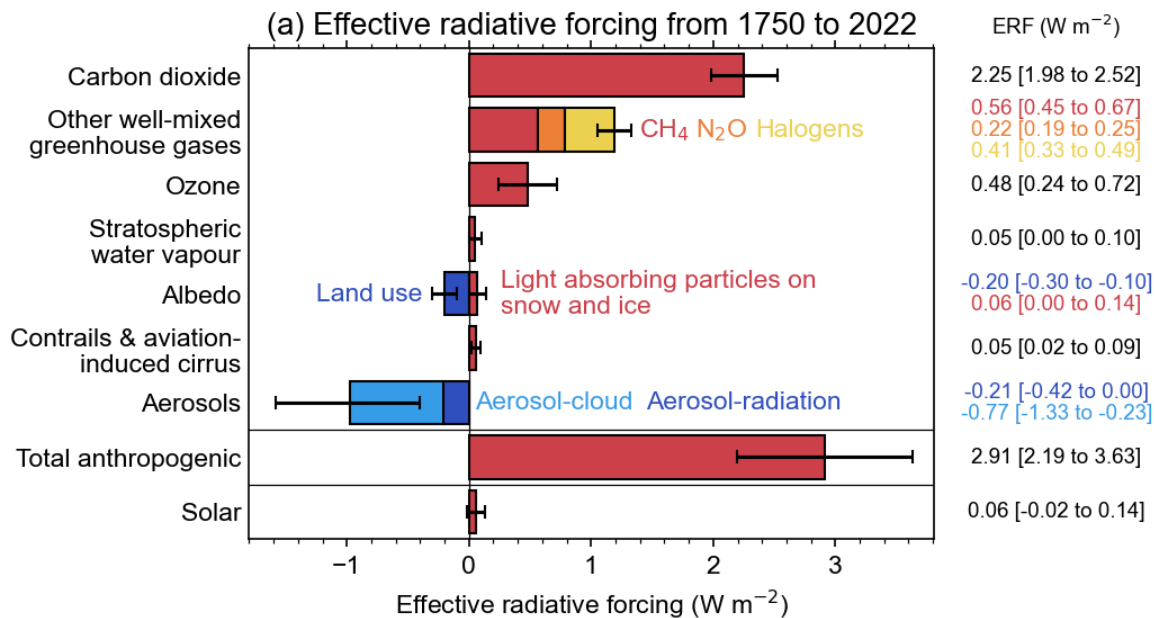
445 Ozone ERF is determined as 0.48 [0.24 to 0.72] W m^{-2} for 1750-2022, similar to the AR6 assessment of 0.47 [0.24 to 0.71] W m^{-2} for 1750-2019. Land use forcing and stratospheric water vapour from methane oxidation are unchanged (to two decimal places) since AR6. The decline in BC emissions from 2019 to 2022 has reduced ERF from light absorbing particles on snow and ice from 0.08 [0.00 to 0.18] W m^{-2} for 1750-2019 to 0.06 [0.00 to 0.14] W m^{-2} for 1750-2022. We determine from

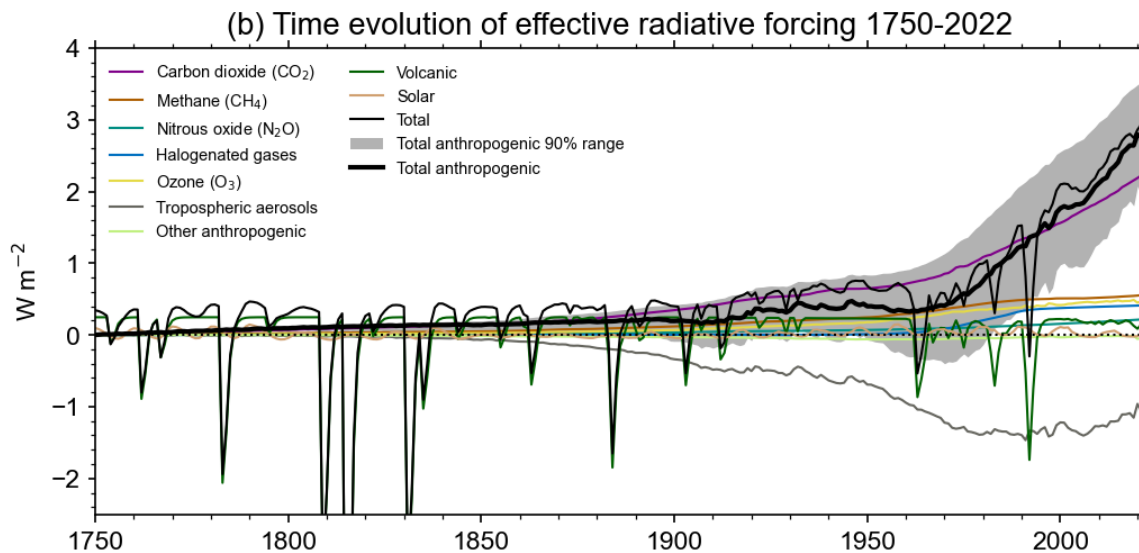
provisional data that aviation activity in 2022 had not yet returned to pre-COVID levels. Therefore, ERF from contrails and
 450 contrail-induced cirrus is lower than AR6, at 0.05 [0.02 to 0.09] W m^{-2} in 2022 compared to 0.06 [0.02 to 0.10] W m^{-2} in 2019.

The headline assessment of solar ERF is unchanged, at 0.01 [-0.06 to +0.08] W m^{-2} from pre-industrial to the 2009-2019 solar
 cycle mean. Separate to the assessment of solar forcing over complete solar cycles, we provide a single year 2022 solar ERF
 of 0.06 [-0.02 to +0.14] W m^{-2} . This is higher than the single year estimate of solar ERF for 2019 (a solar minimum) of -0.02
 455 [-0.08 to 0.06] W m^{-2} .

For volcanic ERF, updating of the pre-industrial dataset for stratospheric aerosol optical depth (sAOD) increased the sAOD
 over 500 BCE to 1749 CE, resulting in a larger difference to post-1750 sAOD and resulting in a volcanic ERF difference of
 +0.015 W m^{-2} compared to AR6 (see Sect. 4 in the Supplementary Material). In addition, the earlier Holocene was more
 460 volcanically active than the period after 500 BCE, further increasing the mean sAOD baseline. Taking the longer baseline
 period into account in the new preindustrial dataset, post-1750 ERF is further increased by 0.031 W m^{-2} . The net effect is that
 volcanic forcing after 1750 has increased by +0.046 W m^{-2} compared to AR6 due to dataset updates and by account of the fact
 that the post-1750 period was less volcanically active on average than the early Holocene which is now used in the ERF
 calculation.

465





470 Figure 2: Effective radiative forcing from 1750-2022. (a) 1750-2022 change in ERF, showing best estimates (bars) and 5-95% uncertainty ranges (lines) from major anthropogenic components to ERF, total anthropogenic ERF, and solar forcing. (b) Time evolution of ERF from 1750 to 2022. Best estimates from major anthropogenic categories are shown along with solar and volcanic forcing (thin coloured lines), total (thin black line) and anthropogenic total (thick black line). 5-95% uncertainty in the anthropogenic forcing is shown in shaded grey. Note solar forcing in 2022 is a single-year estimate.

Table 3: Contributions to anthropogenic effective radiative forcing (ERF) for 1750-2022 assessed in this section.

Forcer	1750-2022 W m ⁻²	1750-2019 (AR6) W m ⁻²	1750-2011(AR5) W m ⁻²	Reason for change from AR6
CO ₂	2.25 [1.98 to 2.52]	2.16 [1.90 to 2.41]	1.82 [1.63 to 2.01]	Increases in GHG concentrations
CH ₄	0.56 [0.45 to 0.67]	0.54 [0.43 to 0.65]	0.48 [0.43 to 0.53]	
N ₂ O	0.22 [0.19 to 0.25]	0.21 [0.18 to 0.24]	0.17 [0.14 to 0.20]	

Halogenated GHGs	0.41 [0.33 to 0.49]	0.41 [0.33 to 0.49]	0.36 [0.32 to 0.40]	
Ozone	0.48 [0.24 to 0.72]	0.47 [0.24 to 0.71]	0.35 [0.21 to 0.67]	Changes in precursor emissions and chemically active GHGs; net effect almost cancels
Stratospheric water vapour	0.05 [0.00 to 0.10]	0.05 [0.00 to 0.10]	0.07 [0.02 to 0.12]	
Aerosol-radiation interactions	-0.21 [-0.42 to 0.00]	-0.22 [-0.47 to 0.04]	-0.45 [-0.95 to 0.05]	Reduction in aerosol and aerosol precursor emissions
Aerosol-cloud interactions	-0.77 [-1.33 to -0.23]	-0.84 [-1.45 to -0.25]	-0.45 [-1.2 to 0.0]	
Land use	-0.20 [-0.30 to -0.10]	-0.20 [-0.30 to -0.10]	-0.15 [-0.25 to -0.05]	
Light-absorbing particles on snow and ice	0.06 [0.00 to 0.14]	0.08 [0.00 to 0.18]	0.04 [0.02 to 0.09]	Reduction in BC emissions
Contrails and aviation-induced cirrus	0.05 [0.02 to 0.09]	0.06 [0.02 to 0.10]	0.05 [0.02 to 0.15]	As of 2022, global aviation activity has not yet returned to pre-COVID19 levels
Total anthropogenic	2.91 [2.19 to 3.63]	2.72 [1.96 to 3.48]	2.3 [1.1 to 3.3]	Increase in GHG concentrations and reduction in aerosol emissions
Solar irradiance	0.01 [-0.06 to 0.08]	0.01 [-0.06 to 0.08]	0.05 [0.0 to 0.10]	

475 All values are in $W m^{-2}$ and 5-95% ranges are in square brackets. As a comparison, the equivalent assessments from AR6 (1750-2019) and AR5 (1750-2011; Myhre et al., 2013b) are shown. Solar ERF is included and unchanged from AR6, based on the most recent solar cycle (2009-2019) thus differing from the single-year estimate in Fig. 2a. Volcanic ERF is excluded due to the sporadic nature of eruptions.

5. Global surface temperature

480

AR6 WGI Chapter 2 assessed the 2001-2020 globally averaged surface temperature change above an 1850-1900 baseline to be 0.99 [0.84 to 1.10] °C and 1.09 [0.95 to 1.20] °C for 2011-2020 (Gulev et al., 2021). Updated estimates to 2022 were also given in AR6 SYR (Lee et al., 2023). The AR6 SYR estimates match those given here. We describe the update in detail and provide further quantification and comparisons.

485

There are choices around the methods used to aggregate surface temperatures into a global average, how to correct for systematic errors in measurements, methods of infilling missing data, and whether surface measurements or atmospheric temperatures just above the surface are used. These choices, and others, affect temperature change estimates and contribute to uncertainty (IPCC AR6 WGI Chapter 2, Cross Chapter Box 2.3, Gulev et al., 2021). The methods chosen here closely follow AR6 WGI and are presented in Supplementary Material, Sect. 5. Confidence intervals are taken from AR6 as only one of the employed datasets regularly updates ensembles (see Supplementary Material, Sect. 5).

490

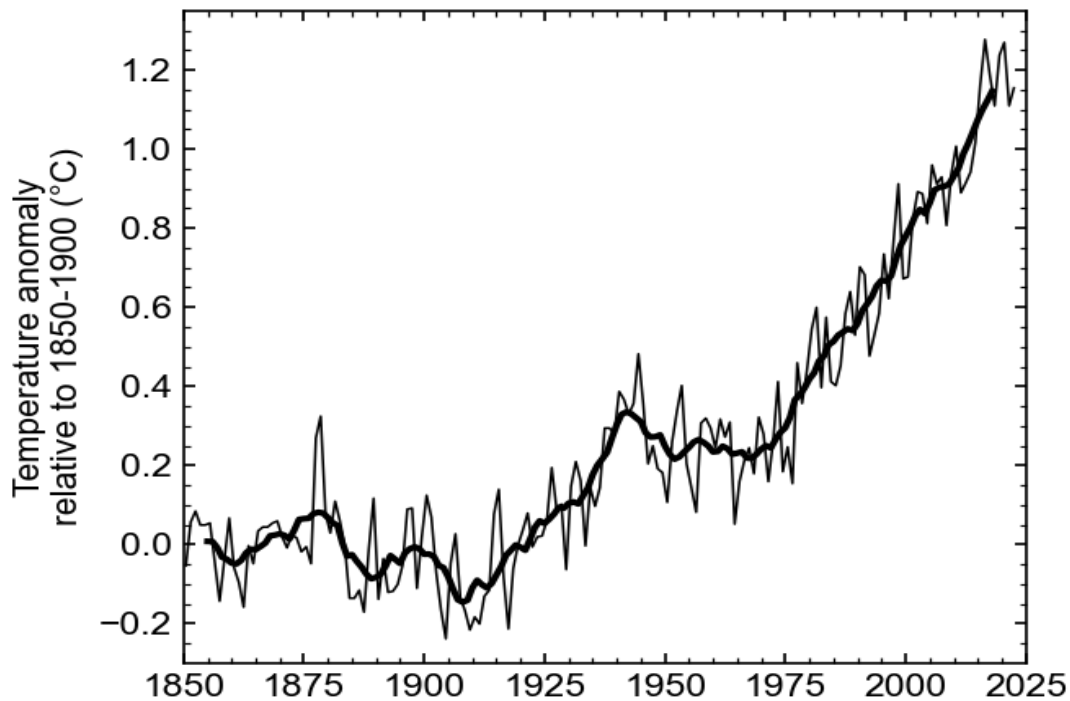
Based on the updates available as of February 2023 (which were reported in the AR6 SYR), the change in global surface temperature from 1850-1900 to 2013-2022, using the same underlying data sets and methodology as AR6, is 1.15 [1.00-1.25] °C, an increase of 0.06 °C within two years from the 2011-2020 value reported in AR6 WGI (Table 4). The change from 1850-1900 to 2003-2022 was 1.03 [0.87-1.13] °C, 0.04 °C higher than the earlier value reported in AR6 WGI. These changes are broadly consistent with typical warming rates over the last few decades, which were assessed in AR6 as 0.76 °C over the 1980-2020 period (using ordinary-least-square linear trends), or 0.019 °C per year (Gulev et al., 2021). They are also broadly consistent with projected warming rates from 2001-2020 to 2021-2040 reported in AR6, which are in the order of 0.025 °C per year under most scenarios (Lee et al., 2021).

500

Table 4: Estimates of global surface temperature change from 1850-1900 [*very likely* (90-100% probability) ranges] for IPCC AR6 and the present study.

Time Period	Temperature change from 1850-1900 (°C)	
	IPCC AR6	This study
Global, most recent 10 years	1.09 [0.95 to 1.20] (to 2011-2020)	1.15 [1.00 to 1.25] (to 2013-2022)

Global, most recent 20 years	0.99 [0.84 to 1.10] (to 2001-2020)	1.03 [0.87 to 1.13] (to 2003-2022)
Land, most recent 10 years	1.59 [1.34 to 1.83] (to 2011-2020)	1.65 [1.36 to 1.90] (to 2013-2022)
Ocean, most recent 10 years	0.88 [0.68 to 1.01] (to 2011-2020)	0.93 [0.73 to 1.04] (to 2013-2022)



505

Figure 3. Annual (thin line) and decadal (thick line) means of global surface temperature (expressed as a change from the 1850-1900 reference period).

Note that the temperatures for single years include considerable variability and are influenced by natural forcings such as the
 510 El Niño-Southern Oscillation and sporadic volcanic eruptions that might either cool or warm the climate for short periods

(Jenkins et al., 2023). At current warming rates individual years may exceed warming of 1.5°C several years before a long-term mean exceeds this level (Trewin, 2022).

6. Earth Energy Imbalance

515 The Earth energy imbalance (EEI) assessed in Chapter 7 of AR6 WGI (Forster et al., 2021), provides a measure of accumulated additional energy (heating) in the climate system, and hence plays a critical role in our understanding of climate change. It represents the difference between the radiative forcing acting to warm the climate and Earth’s radiative response, which acts to oppose this warming. On annual and longer timescales, the Earth heat inventory changes associated with EEI are dominated by the changes in global ocean heat content (OHC), which accounts for about 90% of global heating since the 1970s (Forster et al., 2021). This planetary heating results in changes to the Earth system such as sea level rise, ocean warming, ice loss, rise
520 in temperature and water vapour in the atmosphere, and permafrost thawing (e.g., Cheng et al., 2022; von Schuckmann et al., 2023a), with adverse impacts for ecosystems and human systems (Douville et al., 2021; IPCC, 2022).

On decadal timescales, changes in global surface temperatures (Sect. 5) can become decoupled from EEI by ocean heat rearrangement processes (e.g., Palmer and McNeall, 2014; Allison et al., 2020). Therefore, the increase in the Earth heat
525 inventory provides a more robust indicator of the rate of global change on interannual-to-decadal timescales (Cheng et al., 2019; Forster et al., 2021; von Schuckmann et al., 2023a). AR6 WGI found increased confidence in the assessment of changes in the Earth heat inventory compared to previous IPCC reports due to observational advances and closure of the energy and global sea level budgets (Forster et al., 2021; Fox-Kemper et al., 2021).

530 AR6 estimated with that EEI increased from 0.50 [0.32-0.69] W m⁻² during the period 1971-2006 to 0.79 [0.52-1.06] W m⁻² during the period 2006-2018 (Forster et al., 2021). The contributions to increases in the Earth heat inventory throughout 1971-2018 remained stable: 91% for the full-depth ocean; 5% for the land; 3% for the cryosphere and about 1% for the atmosphere (Forster et al., 2021). The increase in EEI (Figure 4) has also been reported by (Cheng et al. 2019; von Schuckmann et al., 2020; 2023a; Loeb et al., 2021; Hakuba et al., 2021; Kramer et al., 2021; Raghuraman et al., 2021). Drivers for the most recent
535 period (i.e., past two decades) are both the increases in effective radiative forcing (Sect. 4) as well as climate feedbacks, such as cloud and sea ice changes. The degree of contribution from the different drivers are uncertain and still under active investigation.

While changes in EEI have been effectively monitored at the top-of-atmosphere by satellites since the mid-2000s, we rely on
540 estimates of OHC change to determine the absolute magnitude of EEI, and its evolution on inter-annual to multi-decadal time

series. The AR6 assessment of ocean heat content change for the 0-2000 m layer was based on global annual mean time series from five ocean heat content datasets: IAP (Cheng et al., 2017); Domingues et al., (2008); EN4 (Good et al., 2013); Ishii et al., (2017); NCEI (Levitus et al., 2012). Four of these datasets routinely provide updated OHC time series for the BAMS State of the Climate report, and all are used for the GCOS Earth heat inventory (von Schuckmann et al., 2020; 2023a) and the annual
545 WMO global state of the climate. The uncertainty assessment for the 0-2000 m layer used the ensemble method described by Palmer et al. (2021) that separately accounts for *parametric* and *structural* uncertainty. The >2000 m OHC change and associated uncertainty was assessed based on trend analysis of the available hydrographic data following Purkey and Johnson (2010). All five of the datasets used for the 0-2000 m OHC assessment are now updated at least annually and should in principle support an AR6 assessment time series update within the first few months of each year. There is potential to increase the
550 observational ensemble used in the assessment by supplementing this set with additional data products that are also available annually for future updates. There is also a potential to update the uncertainty estimate after a more comprehensive understanding of the error sources.

Estimates of EEI should also account for the other elements of the Earth heat inventory, i.e., the atmospheric warming, the
555 latent heat of global ice loss, and heating of the continental land surface (Forster et al., 2021; Cuesta-Valero et al., 2021; 2022; Steiner et al., 2020; Nitzbon et al., 2022a; Vanderkelen et al., 2020; Adusumilli et al., 2022). Some of these components of the Earth heat inventory are routinely updated by a community-based initiative reported in von Schuckmann et al. (2020; 2023a). However, in the absence of annual updates to all heat inventory components, a pragmatic approach is to use recent OHC change as a proxy for EEI, scaling the value up as required based on historical partitioning between Earth system components.

560

We carry out an update to the AR6 estimate of changes in the Earth heat inventory based on updated observational time series for the period 1971-2020 (Table 5 and Figure 4). Time series of heating associated with loss of ice and warming of the atmosphere and continental land surface are obtained from the recent Global Climate Observing System (GCOS) initiative (von Schuckmann et al., 2023b; Adusumilli et al., 2022; Cuesta-Valero et al., 2023; Vanderkelen and Thiery, 2022; Nitzbon
565 et al., 2022b; Kirchengast et al., 2022). We use the original AR6 time series ensemble OHC time series for the period 1971-2018 and then switch to a smaller four-member ensemble for the period 2019-2022. We “splice” the two sets of time series by adding an offset as needed to ensure that the 2018 values are identical. The AR6 heating rates and uncertainties for the ocean below 2000 m are assumed to be constant through the period. The time-evolution of the Earth heat inventory is determined as a simple summation of time series of: atmospheric heating; continental land heating; heating of the cryosphere; and heating of
570 the ocean over three depth layers: 0-700 m, 700-2000 m, and below 2000 m (Figure 4a). While von Schuckmann et al. (2023a) have also quantified heating of permafrost and inland lakes and reservoirs, these additional terms are very small and are omitted here for consistency with AR6 (Forster et al., 2021).

575 A full propagation of uncertainties across all heat inventory components depends on the specific choice of time-period and
different estimates are not directly comparable. Therefore, we take a simple pragmatic approach, using the total ocean heat
content uncertainty as a proxy for the total uncertainty, since this term is two orders of magnitude larger than the other terms
(Forster et al., 2021). To provide estimates of the EEI up to the year 2022, we scale up the values of OHC change in 2021 and
2022 to reflect the about 90% contribution of the ocean to changes in the Earth heat inventory. The EEI is then simply computed
580 as the difference in global energy inventory over each period, converted to units of $W m^{-2}$ using the surface area of the Earth
and the elapsed time. The uncertainties in the global energy inventory for the end-point years are assumed to be independent
and added in quadrature, following the approach used in AR6 (Forster et al., 2021).

Table 5: Estimates of the Earth energy imbalance (EEI) for AR6 and the present study

Time Period	Earth energy imbalance ($W m^{-2}$)	
	Square brackets are [90 % confidence intervals]	
	IPCC AR6	This study
1971-2018	0.57 [0.43 to 0.72]	0.57 [0.43 to 0.72]
1971-2006	0.50 [0.32 to 0.69]	0.50 [0.31 to 0.68]
2006-2018	0.79 [0.52 to 1.06]	0.79 [0.52 to 1.07]
1975-2022	-	0.65 [0.48 to 0.81]
2010-2022	-	0.89 [0.63 to 1.15]

585 In our updated analysis, we find successive increases in EEI for each 20-year period since 1973, with an estimated value of
 0.44 [0.05 to 0.83] W m^{-2} during 1973-1992 that almost doubled to 0.82 [0.60 to 1.04] W m^{-2} during 2003-2022 (Figure 4b). In
 addition, there is some evidence that the warming signal is propagating into the deeper ocean over time, as seen by a robust
 increase of deep (700-2000m) ocean warming since the 1990s (Cheng et al. 2019, 2022). The model simulations qualitatively
 agree with the observational evidence (e.g. Gleckler et al., 2016; Cheng et al. 2019), further suggesting more than half of the
 590 OHC increase since the late 1800s occurs after the 1990s. For 1973-1992 the contribution by ocean vertical layer was 66%,
 28% and 1% for 0-700 m, 700-2000 m and >2000 m, respectively. During 2013-2022 the corresponding layer contributions
 were 50%, 33% and 8%.

The update of the AR6 assessment periods to end in 2022 results in systematic increases of EEI of 0.08 W m^{-2} for 1975-2022
 595 relative to 1971-2018 and 0.10 W m^{-2} for 2010-2022 relative to 2006-2018 (Table 5).

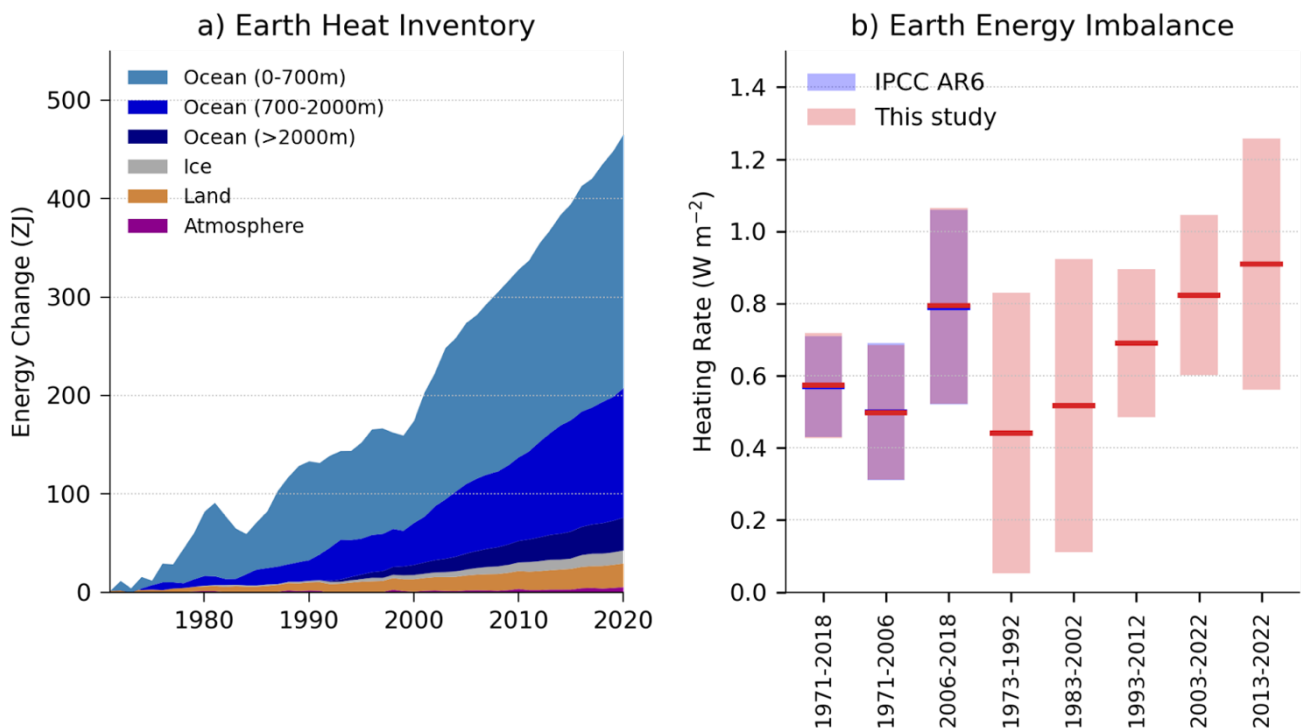


Figure 4: a) Observed changes in the Earth heat inventory for the period 1971-2020 with component contributions as indicated in the figure legend; b) Estimates of the Earth energy imbalance for IPCC AR6 assessment periods, for consecutive twenty-year

600 periods, and the most recent decade. Shaded regions indicate the *very likely* range (90% to 100% probability). Data use and approach are based on the AR6 methods, and further described in Sect. 6.

7 Human-induced global warming

Human-induced warming, also known as anthropogenic warming, refers to the component of observed global surface temperature increase over a specific period (for instance, from 1850-1900 as a proxy for pre-industrial climate to the last 605 decade) attributable to both the direct and indirect effects of human activities, which are typically grouped as follows: well-mixed greenhouse-gases (consisting of CO₂, CH₄, N₂O, and F-gases), and other-human forcings (consisting of aerosol radiation interaction, aerosol cloud interaction, black carbon on snow, contrails, ozone, stratospheric H₂O, and land use) (Eyring et al., 2021). While *total warming*, the actual observed temperature change potentially resulting from both natural climate variability (internal variability of the climate system, and the climate response to natural forcing) and human influences, is the quantity 610 directly related to climate impacts and therefore relevant for adaptation, mitigation efforts focus on human-induced warming as the more relevant indicator for tracking progress against climate stabilisation targets. Further, as the attribution analysis allows to disentangle human-caused warming from possible contributions from solar and volcanic forcing and internal variability (e.g. related to El Niño/La Niña events), it avoids misperception about short-term fluctuations in temperature. An assessment of human-induced warming was therefore provided in two reports within the IPCC's 6th assessment cycle: first in 615 SR1.5 in 2018 (Chapter 1 Sect. 1.2.1.3 and Figure 1.2 (Allen et al., 2018), summarised in SPM A.1 and Figure SPM.1 (IPCC, 2018)) and second in AR6 in 2021 (WGI Chapter 3 Sect. 3.3.1.1.2 and Figure 3.8 (Eyring et al., 2021), summarised in WGI SPM A.1.3 and Figure SPM.2 (IPCC, 2021b)).

7.1.1 Warming period definitions in the IPCC Sixth Assessment Cycle

AR6 defined the current human-induced warming relative to the 1850-1900 baseline as the decade-average of the previous 10- 620 year period (see AR6 WGI Chapter 3). This paper provides an update of the 2010-2019 period used in the AR6 to the 2013–2022 decade. SR1.5 defined current human-induced warming as the average of a 30-year period centred on the current-year assuming the recent rate of warming continues (see SR1.5 Chapter 1). This definition is currently almost identical to the present-day single-year value of human-induced warming, differing by about 0.01°C (see results in Sect. 7.4); the attribution assessment in SR1.5 was therefore provided as single-year warming. This section also updates the SR1.5 single-year approach 625 by providing a year 2022 value.

7.1.2 Estimates of global surface temperature: GMST and GSAT

AR6 WGI (Chapter 2 Cross-Chapter Box 2.3, Gulev et al., 2021) described how global mean surface air temperature (GSAT), as is typically diagnosed from climate models, is physically distinct from the global mean surface temperature (GMST)

630 estimated from observations, which generally combine measurements of near-surface temperature over land, and in some cases
over ice, with measurements of sea surface temperature over the ocean. Based on conflicting lines of evidence from climate
models, which show stronger warming of GSAT compared to GMST, and observations, which tend to show the opposite,
Gulev et al. (2021) assessed with *high confidence* that long-term trends in the two indicators differ by less than 10%, but that
there is *low confidence* in the sign of the difference in trends. Therefore, with *medium* confidence, in AR6 WGI Chapter 3
(Eyring et al., 2021), the best estimates and *likely* ranges for attributable warming expressed in terms of GMST were assessed
635 to be equal to those for GSAT, with the consequence that the AR6 warming attribution results can be interpreted as both GMST
and GSAT. While, based on the WGI Chapter 2 (Gulev et al., 2021) assessment, WGI Chapter 3 (Eyring et al., 2021) treated
estimates of attributable warming in GSAT and GMST from the literature together, without any rescaling, we note that climate-
model based estimates of attributable warming in GSAT are expected to be systematically higher than corresponding estimates
of attributable warming in GMST (see e.g. Cowtan et al., 2015; Richardson et al., 2018; Beusch et al., 2020; Gillett et al.,
640 2021). Therefore, given an opportunity to update these analyses from AR6, it is more consistent, and more comparable with
observations of GMST, to report attributable changes in GMST using all three methods (described in Sect. 7.2). The SR1.5
assessment of attributable warming was given in terms of GMST, which is continued here. In line with Sect. 2 and AR6 WGI,
we adopt GMST as the estimate of global surface temperature.

7.2 Methods

645 Both SR1.5 and AR6 drew on evidence from a range of literature for their assessments of human-induced warming, before
selecting results from a smaller subset to produce a quantified estimate. While both the SR1.5 and AR6 assessments used the
latest Global Warming Index (GWI) results (Haustein et al., 2017), AR6 also incorporated results from two other methods,
Regularised Optimal Fingerprinting (ROF) (as in Gillett et al., 2021) and Kriging for Climate Change (KCC) (as in Ribes et
al., 2021). In AR6, all three methods gave results consistent not only with each other, but also results from AR6 WGI Chapter
650 7 (see WGI Chapter 7 Supplementary Material (Smith et al., 2021); Figure 3.8 of AR6 WGI Chapter 3 (Eyring et al., 2021);
and Supplementary Material Sect. 7 Figure S7.1), though the results from Chapter 7 were not included in the AR6 WGI final
calculation because they were not statistically independent. Of the methods used, two (Gillett et al., 2021; Ribes et al., 2021)
relied on CMIP6 DAMIP (Gillett et al., 2016) simulations which ended in 2020, and hence require modifications to update to
the most recent years. The other two methods (Haustein et al., 2017; Smith et al., 2021) are updatable, and can also be made
655 consistent with other aspects of the AR6 assessment and methods. The three methods used in the final assessment of
contributions to warming in AR6 are used again with revisions for this annual update, and are presented in Supplementary
Material, Sect. 7 with any updates to their approaches described in Sect. 7.2.

7.3 Updated estimates of human-caused warming to date

7.3.1 Updated estimate using the AR6 WGI methodology

660 Factoring in results from all three methods, AR6 WGI Chapter 3 (Eyring et al., 2021) defined the *likely* (66% - 100%
probability interval) range for each warming component as the smallest 0.1°C-precision range that enveloped the 5th to 95th
percentile ranges of each method. In addition, a best estimate was provided for the human-induced (Ant) warming component,
calculated as the mean of the 50th percentile values for each method. Best estimates were not provided in AR6 for the other
components (well-mixed greenhouse gases (GHG), other human forcings (OHF), natural forcings (Nat)), with their values in
665 AR6 WGI Figure SPM.2(b) simply being given as the midpoint between the lower and upper bound of the *likely* range, and
therefore not directly comparable with the central values given for human-induced and observed warming. In order to make a
meaningful and consistent comparison, and provide meaningful insight into interannual changes, an improvement is made in
this update: the multi-method-mean best estimate approach is extended for all warming components.

7.3.2 Updated estimate using the SR1.5 methodology applied to the AR6 WGI datasets

670 While a variety of literature was drawn upon for the assessment of human-induced warming in SR1.5 Chapter 1 (Allen et al.,
2018), only one method, the Global Warming Index (GWI), was used to provide a quantitative assessment of the 2017,
'present-day', level of human-induced warming. The latest results for this method were provided in Hausteine et al. 2017, which
gave a central estimate for human-induced warming in 2017 of 1.01°C with 5-95% range of (0.87°C to 1.22°C). SR1.5 then
accounted for methodological uncertainty by rounding this value to 0.1°C precision for its final assessment of 1.0°C and
675 assessing the 0.8°C to 1.2°C range as a *likely* range. No assessment of the contributions from other components was provided
due to limitations in the GWI approach at the time.

While it is possible to continue the SR1.5 assessment approach of using a single method (GWI) rounded to 0.1°C-precision,
for the purpose of providing annual updates this is insufficient; (i) 0.1°C-precision is too coarse to capture meaningful inter-
680 annual changes to the level of present-day warming, (ii) using different selections of methods prevents meaningful comparison
between the results for *decadal mean* and *present-day* warming calculations, and (iii) using the mean of multiple methods
increases the robustness of the results. These points are simultaneously addressed in this update by adopting the latest multi-
method assessment approach, as established in WGI AR6, for both the AR6 *decadal mean* warming update and the SR1.5
present-day single-year warming update. Further, where SR1.5 only provided an assessment for human-induced warming,
685 updates in available attribution methods since SR1.5 mean that it is now also possible to provide a fully-consistent assessment
for all warming components. As with the attribution assessment in SR1.5, this update reports values in Table 6(b) for *single-*

year *present-day* attributable warming, (as discussed in Sect. 7.1.1), with a comparison to results calculated using the SR1.5 trend based definition also provided below in Sect. 7.4.

7.4 Results

690 Results are summarised in Table 6 and Figure 5. WGI AR6 results for 2010-2019 are quoted in Table 6(a), compared with a repeat calculation using updated methods and datasets, and finally updated for the 2013-2022 period. Results from SR1.5 are quoted in Table 6(b) for the 2017 level of human-induced warming, compared with a repeat calculation using the updated selection of methods and datasets (see Sect. 7.2) and the WGI AR6 multi-method assessment approach (see Sect. 7.3.2), and finally updated for 2022. Method-specific contributions to the assessment results, along with timeseries, are given in
695 Supplementary Material Sect. 7.


The repeat calculations for attributable warming in 2010-2019 exhibit good correspondence with the results in WGI AR6 for the same period, (see also Supplementary Material Sect. 7), with an exact correspondence in the best estimate and *likely* range of human-induced warming (Ant).



700

The repeat calculation for the level of attributable anthropogenic warming in 2017 is about 0.1°C larger than the estimate provided in SR1.5 for the same period, resulting from changes in methods and observational data (see above). The updated results for warming contributions in 2022 are also higher than in 2017 due to five additional years of anthropogenic forcing. A repeat assessment using the SR1.5 trend-based definition (see Sect. 7.1.1) leads to results that are very similar to the single-
705 year results reported in Table 6(b), with 0.02°C differences at most.

The attribution assessment in WGI AR6 concluded that, averaged for the 2010-2019 period, all observed warming was human-induced, with solar and volcanic drivers and internal climate variability estimated not to make a contribution. This conclusion remains the same for the 2013-2022 period. Generally, whatever methodology is used, the best estimate of the human-caused
710 warming to date is (within small uncertainties) equal to the observed warming to date.

Table 6: Updates to assessments in the 6th IPCC assessment cycle of warming attributable to multiple influences.

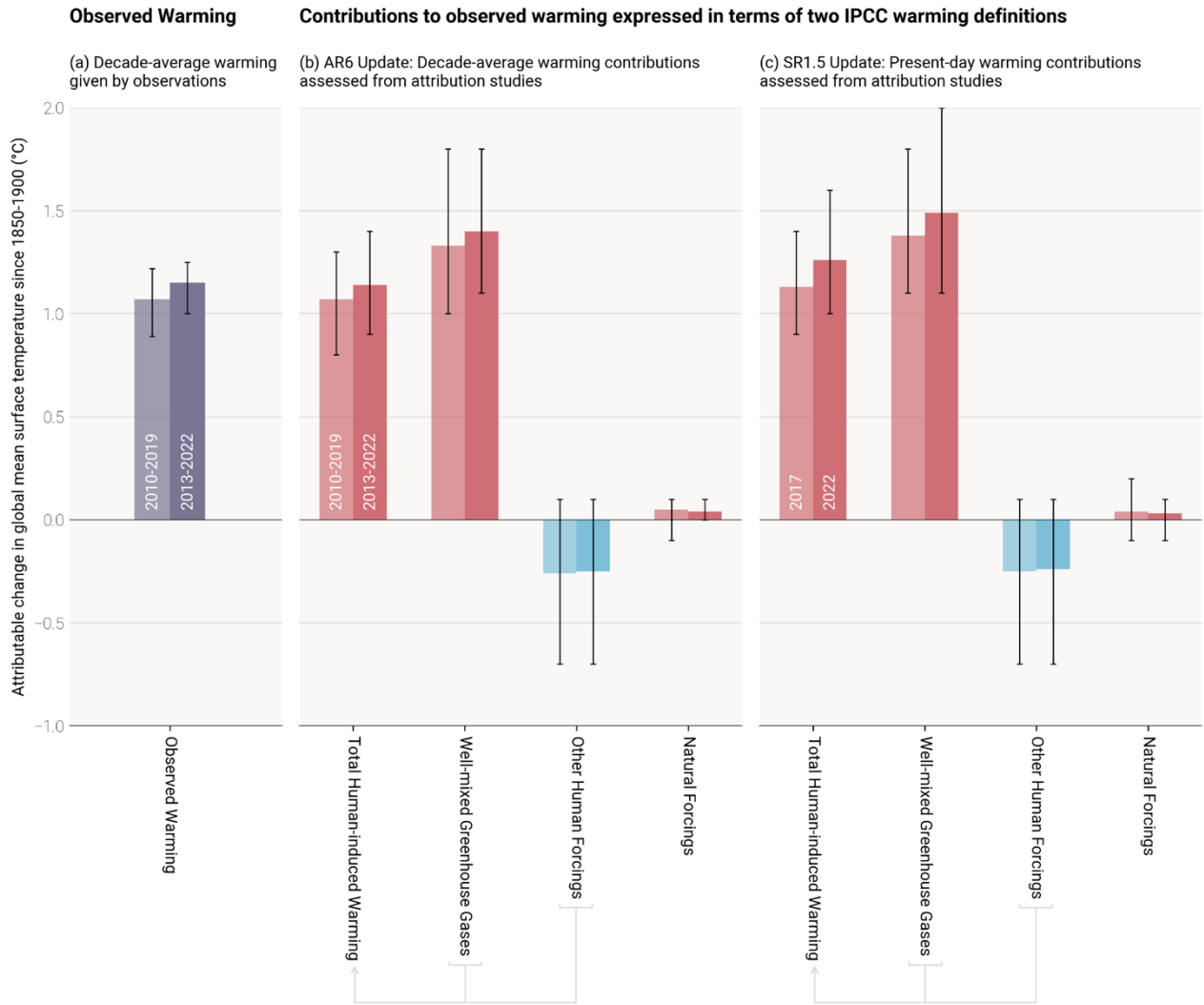
Estimates of warming attributable to multiple influences, in °C, relative to the 1850–1900 baseline period Results are given as best estimates, with the <i>likely</i> range in brackets, and reported as Global Mean Surface Temperature.		
Definition 	(a) IPCC AR6 Attributable Warming Update <i>Average value for previous 10-year period</i>	(b) IPCC SR1.5 Attributable Warming Update <i>Value for single-year period</i>

Period 	(i) 2010-2019 <i>Quoted from AR6 Chapter 3 Sect. 3.3.1.1.2 Table 3.1</i>	(ii) 2010-2019 <i>Repeat calculation using the updated methods and datasets</i>	(iii) 2013-2022 <i>Updated value using updated methods and datasets</i>	(i) 2017 <i>Quoted from SR1.5 Chapter 1 Sect. 1.2.1.3</i>	(ii) 2017 <i>Repeat calculation to using the updated methods and datasets</i>	(iii) 2022 <i>Updated value using updated methods and datasets</i>
Component 						
Observed	1.06 (0.88 to 1.21)	1.07 (0.89 to 1.22) *	1.15 (1.00 to 1.25) *			
Anthropogenic	1.07 (0.8 to 1.3)	1.07 (0.8 to 1.3)	1.14 (0.9 to 1.4)	1.0 (0.8 to 1.2)	1.13 (0.9 to 1.3)	1.26 (1.0 to 1.6)
Well-mixed greenhouse gases	1.40** (1.0 to 2.0)	1.33 (1.0 to 1.8)	1.40 (1.1 to 1.8)	N/A	1.38 (1.1 to 1.8)	1.49 (1.1 to 2.0)
Other human forcings	-0.32** (-0.8 to 0.0)	-0.26 (-0.7 to 0.1)	-0.25 (-0.7 to 0.1)	N/A	-0.25 (-0.7 to 0.1)	-0.24 (-0.7 to 0.1)
Natural forcings	0.03** (-0.1 to 0.1)	0.05 (-0.1 to 0.1)	0.04 (0.0 to 0.1)	N/A	0.04 (-0.1 to 0.2)	0.03 (-0.1 to 0.1)

Results from the 6th IPCC assessment cycle, for both AR6 and SR1.5, are quoted in columns labelled (i), and are compared with repeat calculations in columns labelled (ii) for the same period using the updated methods and datasets to see how methodological and dataset updates alone would change previous assessments. Assessments for the updated periods are reported in columns labelled (iii). Table 6.1(a): * Updated GMST observations, quoted from Sect. 5 of this update, are marked with an asterisk, with very likely ranges given in brackets. ** In AR6 WGI, best estimate values were not provided for warming attributable to well-mixed greenhouse gases, other human forcings, and natural forcings, (though they did receive a likely range, as discussed in Sect. 7.3.1); for comparison, best estimates (marked with two asterisks) have been retrospectively calculated in an identical way to the best estimate that AR6 provided for anthropogenic warming.

715

720



725 **Figure 5: Updated assessed contributions to observed warming relative to 1850-1900, cf. AR6 WGI SPM.2. Results for all time**
periods in this figure are calculated using updated datasets and methods. The 2010-2019 *decade-average* assessed results repeat the
AR6 2010-2019 assessment, and the 2017 *single-year* assessed results repeat the SR1.5 2017 assessment. For each double bar the
lighter and darker shading refers to the earlier and later period respectively. The 2013-2022 *decade-average* and 2022 *single-year*
results are the updated assessments for AR6 and SR1.5 respectively. Panel (a) shows updated observed global warming from Sect.
5, expressed as total GMST, due to both anthropogenic and natural influences. Whiskers give the *very likely* range. Panel (b) and
730 **Panel (c) show updated assessed contributions to warming, expressed as global mean surface temperature, from natural forcings**
and total human-induced forcings, which in turn consists of contributions from well-mixed greenhouse-gases, and other human
forcings. Whiskers give the *likely* range.

8 Remaining carbon budget

735 AR6 assessed the remaining carbon budget (RCB) in Chapter 5 of its WGI report (Canadell et al., 2021) for 1.5°C, 1.7°C and
740 2°C thresholds (see Table 7). They were also reported in its Summary for Policy Makers (Table SPM2, IPCC, 2021b). These
are updated in this section using the same method with transparently described updates.

AR5 (IPCC, 2013) assessed that global surface temperature increase is close to linearly proportional to the total amount of
740 cumulative CO₂ emissions (Collins et al., 2013). The most recent AR6 report reaffirmed this assessment (Canadell et al., 2021).
This near-linear relationship implies that for keeping global warming below a specified temperature level, one can estimate
the total amount of CO₂ that can ever be emitted. When expressed relative to a recent reference period, this is referred to as the
remaining carbon budget (Rogelj et al., 2018).

745 The RCB is estimated by application of the WGI AR6 method described in Rogelj et al. (2019), which involves the combination
of the assessment of five factors: (i) the most recent decade of human-induced warming, (ii) the transient climate response to
cumulative emissions of CO₂ (TCRE), (iii) the zero emissions commitment (ZEC), (iv) the temperature contribution of non-
CO₂ emissions, and (v) an adjustment term for Earth system feedbacks that are otherwise not captured through the other factors.
AR6 WGI reassessed all five terms (Canadell et al., 2021). The incorporation of factor (v) was further considered by Lamboll
750 and Rogelj (2022).

Of these factors, only factor (i) (human-induced warming), where AR6 WGI used the decade-long period, 2010-2019, lends
itself to a regular and systematic annual update. Historical CO₂ emissions from the middle of this period until the start of the
RCB are required to have an as up-to-date RCB estimate as possible.

755 Other factors can be updated but depend on new evidence and insights being published rather than an additional year of
observational data becoming available. Factor (iv) (temperature contribution of non-CO₂ emissions) depends both on the
available mitigation scenario evidence and the assessment of non-CO₂ warming. Additional scenario evidence has become
available through the publication of the scenario database supporting the AR6 WGIII report (Byers et al., 2022) which is taken
760 into account in this update.

The RCB for 1.5°C, 1.7°C and 2°C warming levels are re-assessed based on the most recent available data. Estimated RCBs
are reported below. They are expressed both relative to 2020 to compare to AR6 and relative to the start of 2023 for estimates
based on the 2013-2022 human-induced warming update. Note that between the start of 2020 and the end of 2022, about 122

765 GtCO₂ have been emitted (Sect. 2). Based on the variation in non-CO₂ emissions across the scenarios in AR6 WGIII scenario
 database, the estimated RCB values can be higher or lower by around 200 GtCO₂ depending on how deeply non-CO₂ emissions
 are reduced. The impact of non-CO₂ emissions on warming includes both the warming effects of other greenhouse gases such
 as methane and the cooling effects of aerosols such as sulphates. The impacts of these are assessed using a climate emulator
 (MAGICC, Meinshausen et al., 2011), which was updated to capture recent updates more accurately from the AR6 WGIII
 770 report, but whose results were not captured in the AR6 WGI carbon budget estimates. This emulator update increased the
 estimate of the importance of aerosols, which are expected to decline with time in low emissions pathways (Rogelj et al.,
 2014), causing a net warming, and decreasing the remaining carbon budget. The AR6 WGII version of MAGICC is used here.
 If instead, the FaIR emulator were used, this would give reduced non-CO₂ warming and a larger carbon budget (Lamboll and
 Rogelj, 2022).

775

Table 7: Updated estimates of the Remaining Carbon Budget for 1.5°C, 1.7°C and 2.0°C, for five levels of likelihood, considering only uncertainty in TCRE.

Historical cumulative CO ₂ emissions (1850 - 2019) AR6 WGI Table SPM.2	2390 (± 240; <i>likely</i> (66%-100% probability) range)					
Remaining carbon budgets Case / update	Base year	Estimated remaining carbon budgets from the beginning of base year (GtCO ₂)				
Likelihood of limiting global warming to temperature limit.		17%	33%	50%	67%	83%
1.5°C from AR6 WGI	2020	900	650	500	400	300
+ AR6 emulator update	2020	750	500	400	300	200
+ as above with AR6 scenario update	2020	750	500	400	300	200
+ as above with warming update (2013-2022) (best estimate)	2023	500	300	250	150	100
1.7°C from AR6 WGI	2020	1450	1050	850	700	550
+ AR6 emulator update	2020	1250	900	700	600	450
+ as above with AR6 scenario update	2020	1300	950	750	600	500
+ as above with warming update (2013-2022) (best estimate)	2023	1100	800	600	500	350

2°C from AR6 WGI	2020	2300	1700	1350	1150	900
+ AR6 emulator update	2020	2050	1500	1200	1000	800
+ as above with AR6 scenario update	2020	2200	1650	1300	1100	900
+ as above with warming update (2013-2022) (best estimate)	2023	2000	1450	1150	950	800

780 Estimates start from AR6 WGI estimates (first row for each warming level), updated with the latest scenario information from AR6 WGIII (from second row for each warming level), and an update of the anthropogenic historical warming which is estimated for the 2013-2022 period (third row for each warming level). Estimates are expressed relative to either the start of year 2020 or 2023. The probability includes only the uncertainty in how the Earth immediately responds to carbon, not long-term committed warming or uncertainty in other emissions. All values are rounded to the nearest 50 GtCO₂.

785 Updated RCB estimates presented in Table 7 for 1.5°C, 1.7°C and 2.0°C of global warming are smaller than AR6, and geophysical and other uncertainties therefore have become larger in relative terms. This is a feature that will have to be kept in mind when communicating budgets. The estimates presented here differ from those presented in the annual Global Carbon Budget (GCB) publications (Friedlingstein et al., 2022a). The GCB updates have previously started from the AR6 WGI estimate and subtracted the latest estimates of historical CO₂ emissions. The RCB estimates presented here consider the same updates in historical CO₂ emissions from the GCB as well as the latest available quantification of human-induced warming to date and a reassessment of non-CO₂ warming contributions.

790 If the single year human-induced warming until 2022 (Sect. 7) was used directly in the RCB calculation, this would lead to similar remaining carbon budgets estimates to those from the decadal average approach used here; the 50% likelihood estimates would be unchanged although other likelihoods alter somewhat because the spread due to TCRE uncertainty starts 5 years later. However, we choose to only show the decadal calculation as this was assessed to be the best estimate for human-induced warming and the method adopted in AR6 WGI.

800 The RCB for limiting warming to 1.5°C is becoming very small. It is important, however, to correctly interpret this information. RCB estimates consider projected reductions in non-CO₂ emissions that are aligned with a global transition to net zero CO₂ emissions. These estimates assume median reductions in non-CO₂ emissions between 2020-2050 of CH₄ (50%) N₂O (25%) and SO₂ (77%). If these non-CO₂ greenhouse gas emission reductions are not achieved the RCB would be smaller (see Supplementary Material Sect. 8). Note that the 50% RCB is expected to be exhausted a few years before the 1.5°C global warming level is reached due to the way it factors future warming from non-CO₂ emissions into its estimate.

9. Examples of climate and weather extremes: maximum temperature over land

805 Climate and weather extremes are among the most visible human-induced climate changes. Within AR6 WGI, a full chapter
was dedicated to the assessment of past and projected changes in extremes on continents (Seneviratne et al., 2021), and the
chapter on ocean, cryosphere and sea level changes also provided assessments on changes in marine heatwaves (Fox-Kemper
et al., 2021). Global indicators related to climate extremes include averaged changes in climate extremes, e.g., the mean
increase of annual minimum and maximum temperatures on land (AR6 WGI Chapter 11, Figure 11.2, Seneviratne et al., 2021)
810 or the area affected by certain types of extremes (AR6 WGI Chapter 11, Box 11.1, Figure 1, Seneviratne et al., 2021; Sippel
et al., 2015). In contrast to global surface temperature, extreme indicators are less established. They are therefore expected to
be subject to improvements, reflecting advances in understanding and better data collection. Indeed, such efforts are planned
within the World Climate Research Programme (WCRP) Grand Challenge on Weather and Climate Extremes, which will
likely inform the next iteration of this study.

815

As part of this first update, we provide an upgraded version of the analysis in Figure 11.2 from Seneviratne et al., 2021. Like
the analysis of global mean temperature, the choice of data sets is based on a compromise on the length of the data record, the
data availability, near-real time updates and long-term support. As the indicator (in its current form) averages over all available
land grid points, the spatial coverage should be high to obtain a meaningful average, which further limits the choice of datasets.
820 The HadEX3 dataset (Dunn et al., 2020), which is used for Figure 11.2 in Seneviratne et al. (2021), is static and does not cover
years after 2018. We therefore additionally include the Berkeley Earth Surface Temperature dataset (building off Rohde et al.
2013), and the fifth generation ECMWF atmospheric reanalysis of the global climate (ERA5; Hersbach et al., 2020). Berkeley
Earth data currently enable an analysis of annual indices up to 2021 while ERA5 is updated daily with a latency of about 5
days (and the final release occurs after 2–3 months).

825

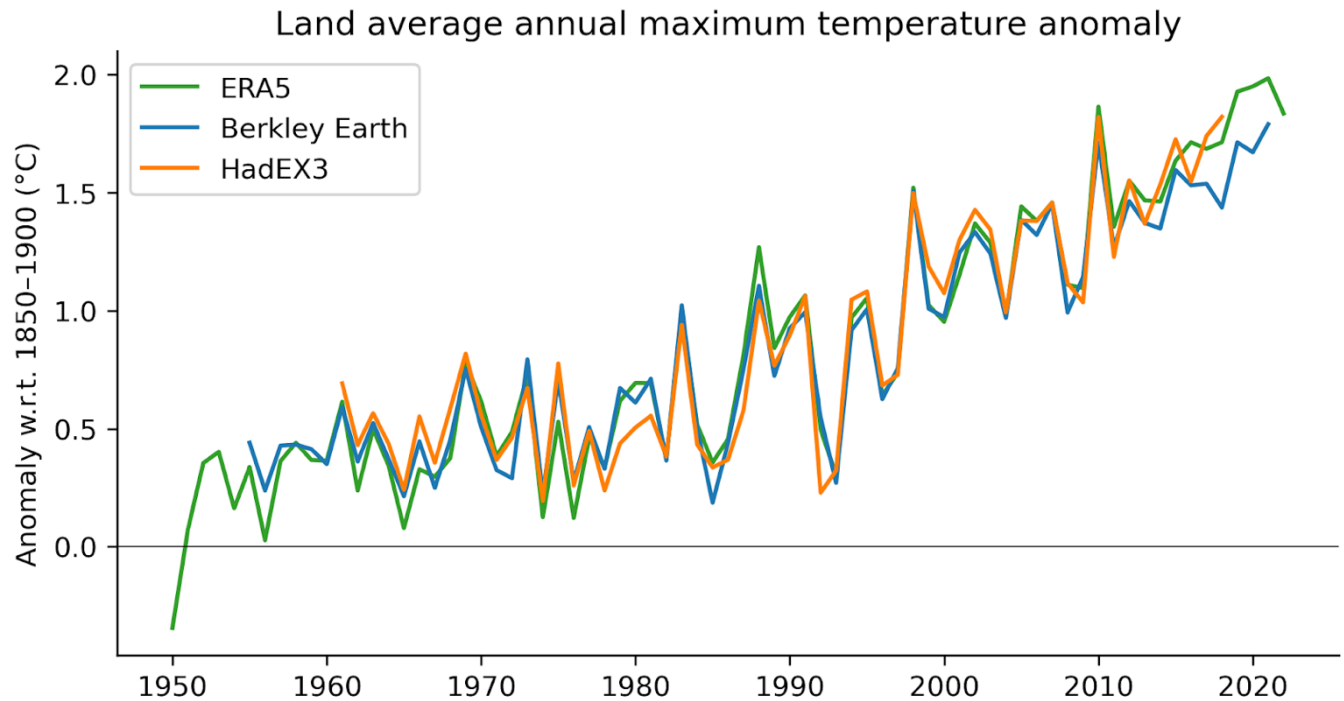
Our proposed climate indicator of changes in temperature extremes consists of land-averaged annual maximum temperatures
(TXx), (excluding Antarctica). For HadEX3 we select the years 1961–2018, to exclude years with insufficient data coverage,
and require at least 90% temporal completeness, thus applying the same criteria as for Figure 11.2 (Seneviratne et al., 2021).
Berkeley Earth provides daily maximum temperatures, and we require more than 99% data availability for each individual
830 year and grid, such that years with more than four missing days are removed. Based on this criterion, Berkeley Earth covers at
least 95% of the global land area from 1955 onwards. ERA5, on the other hand, has full spatiotemporal coverage by design,
and hence the entire currently available period of 1950 to 2022 is used. The annual maximum temperature is then computed
for each grid cell, and a global area-weighted average is calculated for all grid cells with at least 90% temporal completeness
in the respective available period (1955–2021 and 1961–2018 for Berkeley Earth and HadEX3, while ERA5 is again not

835 affected by this criterion). We thus enforce high data availability to adequately calculate global land averaged TXx across all three datasets, but their coverage is not identical which introduces minor deviations in the estimated global land averages. The resulting TXx timeseries are then computed as anomalies with respect to a baseline period of 1961–1990.

To express the TXx as anomalies with respect to 1850-1900 we add an offset to all three datasets. The offset is based on the
840 Berkeley Earth data and is derived from the linear regression of land mean TXx to the annual mean global mean air temperature over the period 1955 to 2020. The offset is then calculated as the slope of the linear regression times the global mean temperature difference between the reference periods 1850-1900 and 1961-1990 (see Supplementary Material, Figure S9.1).

Our climate has warmed rapidly in the last few decades, which also manifests in changes in the occurrence and intensity of
845 climate and weather extremes. We visualise this with land-averaged annual maximum temperatures (TXx) from three different datasets (ERA5, Berkeley Earth and HadEX3), expressed as anomalies with respect to the pre-industrial baseline period of 1850–1900 (Figure 6). From about 1980 onwards, all employed datasets point to a strong TXx increase, which coincides with the transition from global dimming, associated with aerosol increases, to brightening, associated with decreases (Wild et al., 2005). Together with strongly increasing greenhouse gas emissions (Sect. 2), this explains why human-induced climate change
850 has emerged at an even greater pace in the last four decades than previously. For example, land-averaged annual maximum temperatures have warmed by more than 0.5 °C in the past 10 years (1.72 °C with respect to pre-industrial conditions) compared to the first decade of the millennium (1.22 °C; Table 8). Since the offset relative to our pre-industrial baseline period is calculated relative to 1961–1990, within the latter period, temperature anomalies align by construction but can diverge afterwards. In an extensive comparison of climate extreme indices across several reanalyses and observational products, Dunn
855 et al. (2022), point to an overall strong correspondence between temperature extreme indices across reanalysis and observational products, with ERA5 exhibiting especially high correlations to HadEX3 among all regularly updated datasets. This suggests that both our choice of datasets and approach to calculate anomalies does not affect our conclusion — the

intensity of heatwaves across all land areas has unequivocally increased since pre-industrial times.



860 **Figure 6:** Time series of observed temperature anomalies for land average annual maximum temperature (TXx) for ERA5 (1950–2022), Berkeley Earth (1955–2021), and HadEX3 (1961–2018), with respect to 1850–1900. Note that the datasets have different spatial coverage and are not coverage matched. All anomalies are calculated relative to 1961–1990 and an offset of 0.53°C is added to obtain TXx values relative to 1850–1900. Note that while the HadEX3 numbers are the same as shown in Seneviratne et al. (2021) Figure 11.2, these numbers were not specifically assessed.

865 **Table 8:** Anomalies of land average annual maximum temperature (TXx) for recent decades based on HadEX3 and ERA5.

Period	Anomaly w.r.t. 1961-1990 (°C)		Anomaly w.r.t. 1850-1900 (°C)
	HadEX3	ERA5	ERA5
2000-2009	0.72	0.69	1.23
2009-2018	1.01	1.02	1.55
2010-2019	-	1.11	1.64
2011-2020	-	1.12	1.65

2012-2021	-	1.18	1.71
-----------	---	------	------

The anomalies with respect to 1850-1900 are derived by adding an offset of 0.53°C. Note that while the HadEX3 numbers are the same as shown in Seneviratne et al. (2021) Figure 11.2, these numbers were not specifically assessed.

10. Dashboard data visualisations

870 The Climate Change Tracker (<https://climatechangetracker.org/>), a platform hosting a range of publicly available climate data, aims to provide a range of audiences with a reliable, user-friendly means of tracking and understanding climate change and its progression.

875 Building on the existing platform, a bespoke “dashboard” places several of the updated IPCC-consistent indicators of climate change set out above in the public domain. This bespoke dashboard is primarily aimed at policymakers involved in UNFCCC negotiations, but the ultimate intention is to reach and inform a much wider audience.

880 The dashboard initially focuses on three key indicator sets: greenhouse gas emissions (Sect. 2); human-induced global warming (Sect. 7); and the remaining global carbon budget (Sect. 8), bringing together and presenting up-to-date information crucial to effective climate decision-making in a findable, accessible, traceable and reproducible way. In addition, the Climate Change Tracker provides standardised application programming interfaces (APIs), dashboards and charts to embed in third-party apps and websites. All data is traceable to the github repository employed for this paper (Sect. 11).

In time, and with feedback from the user community, the initial set of indicators displayed by the dashboard may be expanded to include others alongside their rates of change.

885 11. Code and data availability

The carbon budget calculation is available from <https://github.com/Rlamboll/AR6CarbonBudgetCalc>. The code and data used to produce other indicators is available in repositories under <https://github.com/ClimateIndicator>. All data is available from <https://doi.org/10.5281/zenodo.7969114> (Smith et al., 2023). Data is provided under a CC-BY 4.0 Licence.

890 **12. Discussion and conclusions**

The first year of the Global Climate Change (IGCC) initiative has built from the AR6 report cycle to provide a comprehensive update of the climate change indicators required to estimate the human induced warming and the remaining carbon budget. Table 9 presents a summary of the headline figures from each section compared to that given in the AR6 assessment. The main substantive data change since AR6 is that land-use CO₂ emissions have been revised down by around 2 GtCO₂. However, as
 895 CO₂ ERF and human induced warming estimates depend on concentrations, not emissions, this does not affect most of the other findings. Note it does slightly increase the remaining carbon budget, but this is only by 5 GtCO₂, less than the 50 GtCO₂ rounding precision.

Table 9: Summary of headline results and methodological updates from the Indicators of Global Climate Change (IGCC) initiative.

Climate Indicator	AR6 2021 assessment	This 2023 assessment	Explanation of changes	Methodological updates
Greenhouse gas emissions AR6 WGIII Chapter 2: Dhakal et al. (2022); see also Minx et al. (2021)	2010-2019 average: 56 ± 6 GtCO ₂ e*	2010-2019 average: 53 ± 5.6 GtCO ₂ e 2012-2021 average: 54 ± 5.3 GtCO ₂ e	The change from AR6 is due to a systematic downward revision in CO ₂ -LULUCF and CH ₄ estimates. Real-world emissions have slightly increased. Average emissions in the past decade grew at a slower rate than in the previous decade. Note following convention, ODS F-gases are excluded from the total.	CO ₂ -LULUCF emissions revised down. PRIMAP-hist used in place of EDGAR for CH ₄ and N ₂ O emissions, atmospheric measurements taken for F-gas emissions. These changes reduce estimates by around 3 GtCO ₂ e (Sect. 2)
Greenhouse gas concentrations AR6 WGI Chapter 2: Gulev et al. (2021)	2019: CO ₂ , 410.1 [± 0.36] ppm CH ₄ , 1866.3 [± 3.2] ppb N ₂ O, 332.1 [± 0.7] ppb	2022: CO ₂ , 417.1 [± 0.4] ppm CH ₄ , 1911.9 [± 3.3] ppb N ₂ O, 335.9 [± 0.4] ppb	Continued and increasing emissions	Updates based on NOAA data as AGAGE not yet available for 2022. To make an AR6-like product, N ₂ O scaled to approximate NOAA-AGAGE average (Sect. 3)
Effective radiative forcing change since 1750	2019: 2.72 [1.96 to 3.48] W m ⁻²	2022: 2.91 [2.19 to 3.63] W m ⁻²	Overall substantial increase and high decadal rate of change, arising from increases in greenhouse gas	Minor update in aerosol precursor method for improved future estimates - had no impact

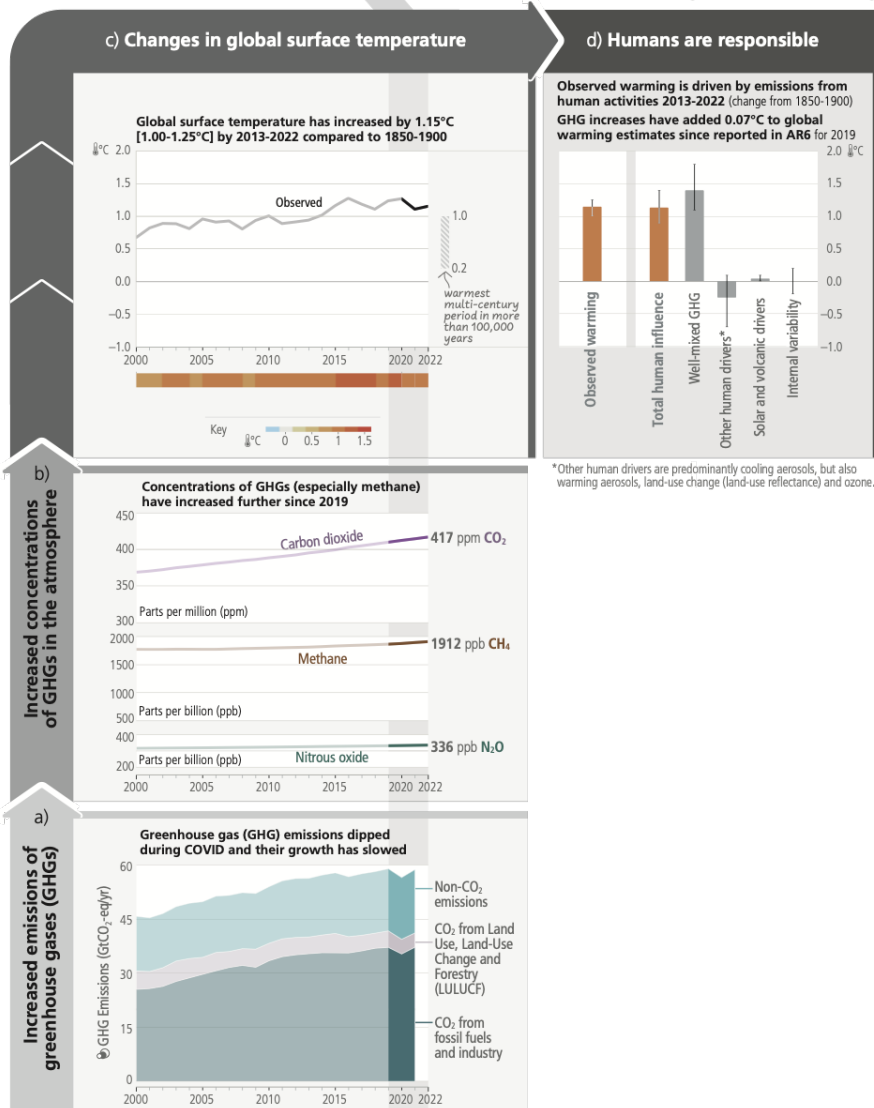
AR6 WGI Chapter 7: Forster et al. (2021)			concentrations and reductions in aerosol precursors	at quoted accuracy level (Sect. 4)
Global mean surface temperature change above 1850-1900 AR6 WGI Chapter 2: Gulev et al. (2021)	2011-2020 average: 1.09 [0.95 to 1.20] °C	2013-2022 average: 1.15 [1.00-1.25] °C	An increase of 0.06 °C within two years, indicating a high decadal rate of change	Methods match AR6 (Sect. 5)
Earth's energy imbalance AR6 WGI Chapter 7: Forster et al. (2021)	2006-2018 average: 0.79 [0.52-1.06] W m ⁻²	2010-2022. average: 0.89 [0.63 to 1.15] W m ⁻²	Substantial increase in energy imbalance estimated based on increased rate of ocean heating.	Ocean heat content timeseries extended from 2018 to 2022 using 4 of the 5 AR6 datasets. Other heat inventory terms updated following von Schuckmann et al (2023). Ocean heat content uncertainty is used as a proxy for total uncertainty. Further details in Sect. 6.
Human induced global warming since preindustrial AR6 WGI Chapter 3: Eyring et al. (2021)	2010-2019 average: 1.07 [0.8 to 1.3] °C	2013-2022 average: 1.14 [0.9 to 1.4] °C	An increase of 0.07 °C within three years, indicating a high decadal rate of change	The three methods for the basis of the AR6 assessment are retained, but each has new input data (Sect. 7)
Remaining carbon budget for 50% likelihood of limiting global warming to 1.5°C AR6 WGI Chapter 5: Canadell et al. (2021)	From the start of 2020: 500 GtCO ₂	From the start of 2023: 250 GtCO ₂	The 1.5°C budget is becoming very small. The RCB can exhaust before the 1.5°C threshold is reached due to having to allow for future non-CO ₂ warming.	Methods match AR6 (Sect. 8)
Land average maximum temperature	2009-2018 average:	2013-2022 average:	Rising at a substantially faster rate compared to global mean surface temperature	HadEX3 data used in AR6 replaced with reanalysis data employed in this report which is more updatable going forward.

<p>change compared to pre-industrial.</p> <p>AR6 WGI Chapter 11: Seneviratne et al., 2021</p>	<p>1.55 °C</p>	<p>1.74 °C</p>		<p>Adds 0.01 °C to estimate (Sect. 9)</p>
-------------------------------------------------------------------------------------------------------------	-----------------------	-----------------------	--	--------------------------------------------------

900

Figure 7 summarises contributions to warming, repeating Figure 2.1 of the AR6 Synthesis Report (Lee et al., 2023). It highlights changes since the assessment period in ARG WGI. Table 9 also summarises methodological updates.

Since AR6 WGI (2021), humans had added to global warming



905 Figure 7. The causal chain from emissions to resulting warming of the climate system. Emissions of GHG have increased rapidly over recent decades (panel a). These emissions have led to increases in the atmospheric concentrations of several GHGs including the three major well-mixed GHGs (panel b). The global surface temperature (shown as annual anomalies from an 1850–1900 baseline) has increased by around 1.15°C since 1850–1900 (panel c). The human-induced warming estimate over the last decade is a close match to the observed warming (panel d). Whiskers show 5% to 95% ranges. Figure is modified from AR6 SYR with a zoom on the period 2000 to 2022 for the upper two panels (Figure 2.1, Lee et al., 2023).

910

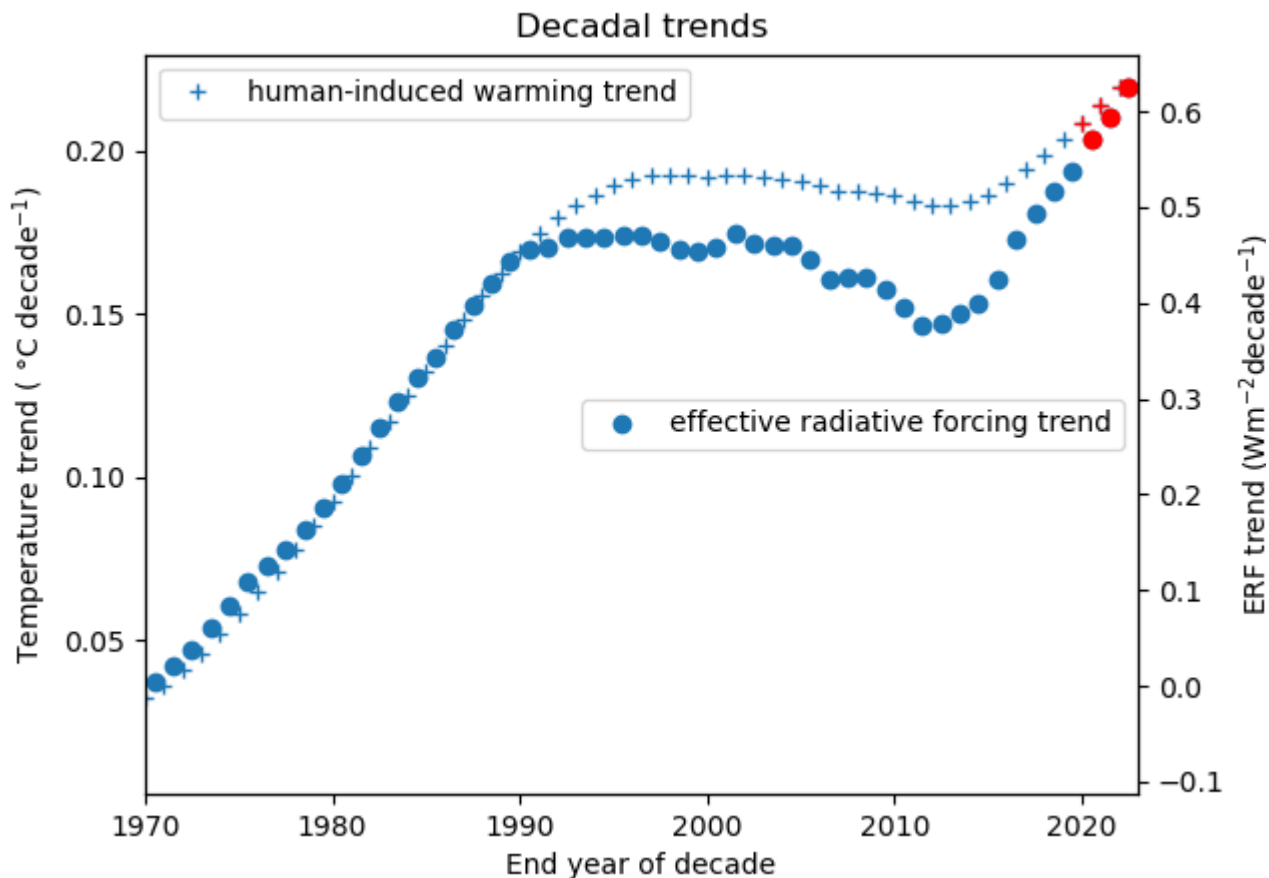
It is hoped that this update can support the science community in its collection and provision of reliable and timely global climate data. In future years we are particularly interested in improving SLCF updating methods to get a more accurate estimate of short-term ERF changes. The work also highlights the importance of high-quality metadata to document changes in methodological approaches over time. In future years we hope to improve the robustness of the indicators presented here but also extend the breadth of indicators reported through coordinated research activities. For example, we could begin to make use of new satellite data inversion techniques to infer recent emissions. We are particularly interested in exploring how we might update indicators of regional climate extremes and their attribution, which are particularly relevant for supporting actions on adaptation and loss and damage.

915
920

Generally, scientists and scientific organisations such as WMO and IPCC have an important role as “watchdogs” to critically inform evidence-based decision making. This annual update traced to IPCC methods can provide a reliable, timely source of trustworthy information. As well as helping inform decisions, we can use the update to track changes in dataset homogeneity between their use in one IPCC report and the next. We can also provide information and testing to motivate updates in methods that future IPCC reports might choose to employ.

Figure 8 shows decadal trends for the attributed warming and ERF. The most recent trends were unprecedented at the time of AR6 and have increased further since then (red markers), showing that human activities are consistently causing global warming recently of more than 0.2 °C per decade. As nations and businesses forge climate policies and take meaningful action, the latest available evidence shows that global actions are not yet at the scale to manifest a substantive shift in the direction of global human influence on the Earth’s energy imbalance and the resulting global warming. Indeed, our results point to the opposite: the evidence shows continued increase in cumulative CO₂ emissions, increased emissions of other GHGs, and gains in air quality at the expense of the loss of the cooling effect from aerosols. Both AR6 WGI and WGIII reports highlighted the benefits of short-term reductions in methane emissions to counter the loss of aerosol cooling and further improve air quality - however, at the global scale, methane emissions are at their highest level and rising (see Table 1). Policy makers, civil society and the scientific community require monitoring data and analyses from rigorous, robust assessments available on a regular basis. These results illustrate how assessments such as ours provide a strong "reality check" based on science and real-world data.

930
935



940

Figure 8: Decadal trends in human-induced warming - left axis, and anthropogenic effective radiative forcing (ERF) - right axis. These are computed from the GlobalWarming Index human-induced warming estimate shown in Supplementary Material Sect. 7 and Figure 2b respectively. The red points mark three additional years since the AR6 time series for these indicators ended in 2019.

945

This is a critical decade: human-induced global warming rates are at their highest historical level and 1.5 °C global warming might be expected to be reached or exceeded within the next 10 years in the absence of cooling from major volcanic eruptions (Lee et al., 2021). Yet this is also the decade that global greenhouse gas emissions could be expected to peak and begin to substantially decline. The indicators of global climate change presented here show that the Earth's energy imbalance has increased to around 0.9 W m⁻², averaged over the last 12 years. This also has implications for the committed response of slow components in the climate system (glaciers, deep ocean, ice sheets) and committed long-term sea level rise but this is not part of the update here. However, rapid and stringent GHG emission decreases could halve warming rates over the next 20 years.

950

(McKenna et al., 2021). Table 1 shows that global GHG emissions are at a long term high, yet there are signs that their rate of increase has slowed. Depending on the societal choices made in this critical decade, a continued series of these annual updates could track a change in direction for the human influence on climate.

955 13. Acknowledgements

Piers Forster, Debbie Rosen, Joeri Rogelj and Robin Lamboll were supported by the EU Horizon 2020 Research and Innovation Programme grant no.820829 (CONSTRAIN). Chris Smith was supported by a NERC/IIASA collaborative research fellowship (NE/T009381/1). Matthew D. Palmer, Colin Morice and Rachel Killick were supported by the Met Office Hadley Centre Climate Programme funded by BEIS. William F. Lamb and Jan C. Minx were supported by the ERC-2020-SyG
960 "GENIE" (grant ID 951542). Pierre Friedlingstein, Glen P. Peters and Robbie M. Andrew were supported by EU Horizon 2020 Research and Innovation Programme grant no. 821003 (4C). HadEX3 [3.0.4] data were obtained from <https://www.metoffice.gov.uk/hadobs/hadex3/> on 05.04.2023 and are © British Crown Copyright, Met Office, 2022, provided under an Open Government Licence <http://www.nationalarchives.gov.uk/doc/open-government-licence/version/2/>.

965 14. Author contributions

PMF, CJS, MA, PF, JR, MRC and AP developed the concept of an annual update in discussions with the wider IPCC community over many years. CJS led the work of the data repositories. A. Borger and JAB led the website development with visualisation support from DR, JMG and A. Birt. VMD, PZ, SS, JM, C-FS, SIS, VN, AP, J-YL, NG, FD, GP, BT, MSP, MRC, JR, PF, MA and PT provided important IPCC and UNFCCC framing. PMF coordinated the production of the manuscript with
970 support from DR. WFL led Sect. 2 with contributions from CJS, JM, PF, GP, JG, JP and RA. CJS led Sects. 3 and 4 with contributions from BH, FD, SS, VN and XL. BT led Sect. 5 with contributions from PT, CM, CK, JK, RR, RV and LC. KvS and MDP led Sect. 6 with contributions from LC, MI, TB and RK. TW led Sect. 7 with contributions and calculations from AR, NG and MR. JR led Sect. 8 with contributions from RL and KZ. Sect. 9 was led by SIS and XC with calculations by MH and DS. All authors either edited or commented on the manuscript.

975 15. Competing interests

The authors declare no competing interests.

References

- Adusumilli, S., Straneo, F., Hendricks, S., Korosov, A., Lavergne, T., Lawrence, I., Marzeion, B., Otsuka, I., Schweiger, A., Shepherd, A., Slater, D., Slater, T., Timmermanns, M.-L., and Zemp, M.: GCOS EHI 1960-2020 Cryosphere Heat Content, https://doi.org/10.26050/WDCC/GCOS_EHI_1960-2020_CRHC, 2022.
- Allen, M. R., O. P. Dube, W. Solecki, F. Aragón-Durand, W. Cramer, S. Humphreys, M. Kainuma, J. Kala, N. Mahowald, Y. MuLugetta, R. Perez, M. Wairiu, and K. Zickfeld, 2018: Framing and Context. In: Global Warming of 1.5°C. An IPCC Special Report on the impacts of global warming of 1.5°C above pre-industrial levels and related global greenhouse gas emission pathways, in the context of strengthening the global response to the threat of climate change, sustainable development, and efforts to eradicate poverty [Masson-Delmotte, V., P. Zhai, H.-O. Pörtner, D. Roberts, J. Skea, P.R. Shukla, A. Pirani, W. Moufouma-Okia, C. Péan, R. Pidcock, S. Connors, J.B.R. Matthews, Y. Chen, X. Zhou, M.I. Gomis, E. Lonnoy, T. Maycock, M. Tignor, and T. Waterfield (eds.)], Cambridge University Press, Cambridge, UK and New York, NY, USA, 49-92, <https://doi.org/10.1017/9781009157940.003>, 2018.
- Allison, L. C., Palmer, M. D., Allan, R. P., Hermanson, L., Liu, C., and Smith, D. M.: Observations of planetary heating since the 1980s from multiple independent datasets, *Environ. Res. Commun.*, 2, 101001, <https://doi.org/10.1088/2515-7620/abbb39>, 2020.
- Basu, S., Lan, X., Dlugokencky, E., Michel, S., Schwietzke, S., Miller, J. B., Bruhwiler, L., Oh, Y., Tans, P. P., Apadula, F., Gatti, L. V., Jordan, A., Necki, J., Sasakawa, M., Morimoto, S., Di Iorio, T., Lee, H., Arduini, J., and Manca, G.: Estimating emissions of methane consistent with atmospheric measurements of methane and $\delta^{13}\text{C}$ of methane, *Atmos. Chem. Phys.*, 22, 15351–15377, <https://doi.org/10.5194/acp-22-15351-2022>, 2022.
- Bellouin, N., Davies, W., Shine, K. P., Quaas, J., Mülmenstädt, J., Forster, P. M., Smith, C., Lee, L., Regayre, L., Brasseur, G., Sudarchikova, N., Bouarar, I., Boucher, O., and Myhre, G.: Radiative forcing of climate change from the Copernicus reanalysis of atmospheric composition, *Earth Syst. Sci. Data*, 12, 1649–1677, <https://doi.org/10.5194/essd-12-1649-2020>, 2020.
- Beusch, L., Gudmundsson, L., and Seneviratne, S. I.: Crossbreeding CMIP6 Earth System Models With an Emulator for Regionally Optimized Land Temperature Projections, *Geophys. Res. Lett.*, 47, <https://doi.org/10.1029/2019GL086812>, 2020.
- Bond, T. C., Doherty, S. J., Fahey, D. W., Forster, P. M., Berntsen, T., DeAngelo, B. J., Flanner, M. G., Ghan, S., Kärcher, B., Koch, D., Kinne, S., Kondo, Y., Quinn, P. K., Sarofim, M. C., Schultz, M. G., Schulz, M., Venkataraman, C., Zhang, H., Zhang, S., Bellouin, N., Guttikunda, S. K., Hopke, P. K., Jacobson, M. Z., Kaiser, J. W., Klimont, Z., Lohmann, U., Schwarz, J. P., Shindell, D., Storelvmo, T., Warren, S. G., and Zender, C. S.: Bounding the role of black carbon in the climate system: A scientific assessment, *J. Geophys. Res.-Atmos.*, 118, 5380–5552, <https://doi.org/10.1002/jgrd.50171>, 2013.

- Byers, E., Krey, V., Kriegler, E., Riahi, K., Schaeffer, R., Kikstra, J., Lamboll, R., Nicholls, Z., Sandstad, M., Smith, C., van der Wijk, K., Lecocq, F., Portugal-Pereira, J., Saheb, Y., Stromann, A., Winkler, H., Auer, C., Brutschin, E., Lepault, C., Müller-Casseres, E., Gidden, M., Huppmann, D., Kolp, P., Marangoni, G., Werning, M., Calvin, K., Guivarch, C., Hasegawa, T., Peters, G., Steinberger, J., Tavoni, M., van Vuuren, D., Al -Khourdajie, A., Forster, P., Lewis, J., Meinshausen, M., Rogelj, J., Samset, B., and Skeie, R.: AR6 Scenarios Database, <https://doi.org/10.5281/ZENODO.5886912>, 2022.
- Canadell, J.G., P. M. S. Monteiro, M. H. Costa, L. Cotrim da Cunha, P. M. Cox, A.V. Eliseev, S. Henson, M. Ishii, S. Jaccard, C. Koven, A. Lohila, P. K. Patra, S. Piao, J. Rogelj, S. Syampungani, S. Zaehle, and K. Zickfeld: Global Carbon and other Biogeochemical Cycles and Feedbacks. In Climate Change 2021: The Physical Science Basis. Contribution of Working Group I to the Sixth Assessment Report of the Intergovernmental Panel on Climate Change [Masson-Delmotte, V., P. Zhai, A. Pirani, S.L. Connors, C. Péan, S. Berger, N. Caud, Y. Chen, L. Goldfarb, M.I. Gomis, M. Huang, K. Leitzell, E. Lonnoy, J.B.R. Matthews, T.K. Maycock, T. Waterfield, O. Yelekçi, R. Yu, and B. Zhou (eds.)]. Cambridge University Press, Cambridge, United Kingdom and New York, NY, USA, pp. 673–816, <https://doi.org/10.1017/9781009157896.007>, 2021.
- Cheng, L., Trenberth, K. E., Fasullo, J., Boyer, T., Abraham, J., and Zhu, J.: Improved estimates of ocean heat content from 1960 to 2015, *Sci. Adv.*, 3, e1601545, <https://doi.org/10.1126/sciadv.1601545>, 2017.
- Cheng, L., Abraham, J., Hausfather, Z., and Trenberth, K. E.: How fast are the oceans warming?, *Science*, 363, 128–129, <https://doi.org/10.1126/science.aav7619>, 2019.
- Cheng, L., Von Schuckmann, K., Abraham, J. P., Trenberth, K. E., Mann, M. E., Zanna, L., England, M. H., Zika, J. D., Fasullo, J. T., Yu, Y., Pan, Y., Zhu, J., Newsom, E. R., Bronselaer, B., and Lin, X.: Past and future ocean warming, *Nat. Rev. Earth. Environ.*, 3, 776–794, <https://doi.org/10.1038/s43017-022-00345-1>, 2022.
- Collins, M., Knutti, R., Arblaster, J., Dufresne, J.-L., Fichet, T., Friedlingstein, P., Gao, X., Gutowski, W.J., Johns, T., Krinner, G., Shongwe, M., Tebaldi, C., Weaver, A.J. & Wehner, M.: Long-term Climate Change: Projections, Commitments and Irreversibility. In: V.B. Stocker T.F., .D. Qin, G.K. Plattner, M. Tignor, S.K. Allen, J. Boschung, A. Nauels, Y. Xia & P.M. Midgley (eds.). Climate Change 2013: The Physical Science Basis. Contribution of Working Group I to the Fifth Assessment Report of the Intergovernmental Panel on Climate Change. Cambridge, United Kingdom and New York, NY, USA, Cambridge University Press. pp. 1029–1136, 2013.
- Cowtan, K., Hausfather, Z., Hawkins, E., Jacobs, P., Mann, M. E., Miller, S. K., Steinman, B. A., Stolpe, M. B., and Way, R. G.: Robust comparison of climate models with observations using blended land air and ocean sea surface temperatures, *Geophys. Res. Lett.*, 42, 6526–6534, <https://doi.org/10.1002/2015GL064888>, 2015.
- Crippa, M., Guizzardi, D., Banja, M., Solazzo, E., Muntean, M., Schaaf, E., Pagani, F., Monforti-Ferrario, F., Olivier, J. G. J., Quadrelli, R., Riskez Martin, A., Taghavi-Moharamli, P., Grassi, G., Rossi, S., Oom, D., Branco, A., San-Miguel, J., Vignati, E.: CO₂ emissions of all world countries: JRC/IEA/PBL 2022 report, Publications Office, LU, <https://doi.org/10.2760/07904>, 2022.

- 1040 Cuesta-Valero, F. J., García-García, A., Beltrami, H., González-Rouco, J. F., and García-Bustamante, E.: Long-term global ground heat flux and continental heat storage from geothermal data, *Clim. Past*, 17, 451–468, <https://doi.org/10.5194/cp-17-451-2021>, 2021.
- Cuesta-Valero, F. J., Beltrami, H., García-García, A., Krinner, G., Langer, M., MacDougall, A. H., Nitzbon, J., Peng, J., von Schuckmann, K., Seneviratne, S. I., Smith, N., Thiery, W., Vanderkelen, I., and Wu, T.: Continental heat storage: Contributions
1045 from ground, inland waters, and permafrost thawing, *Earth Syst. Dynam. Discuss.* [preprint], <https://doi.org/10.5194/esd-2022-32>, 2022.
- Cuesta-Valero, F. J., Beltrami, H., García-García, A., Krinner, G., Langer, M., MacDougall, A., Nitzbon, J., Peng, J., von Schuckmann, K., Seneviratne, S., Thiery, W., Vanderkelen, I., Wu, T.: GCOS EHI 1960-2020 Continental Heat Content (Version 2), World Data Center for Climate (WDCC) at DKRZ, [https://doi.org/10.26050/WDCC/GCOS_EHI_1960-2020_CoHC_v2](https://doi.org/10.26050/WDCC/GCOS_EHI_1960-1050_2020_CoHC_v2), 2023.
- Dhakal, S., J. C. Minx, F. L. Toth, A. Abdel-Aziz, M. J. Figueroa Meza, K. Hubacek, I. G. C. Jonckheere, Yong-Gun Kim, G. F. Nemet, S. Pachauri, X. C. Tan, T. Wiedmann: Emissions Trends and Drivers. In IPCC, 2022: Climate Change 2022: Mitigation of Climate Change. Contribution of Working Group III to the Sixth Assessment Report of the Intergovernmental Panel on Climate Change [P.R. Shukla, J. Skea, R. Slade, A. Al Khourdajie, R. van Diemen, D. McCollum, M. Pathak, S.
1055 Some, P. Vyas, R. Fradera, M. Belkacemi, A. Hasija, G. Lisboa, S. Luz, J. Malley, (eds.)]. Cambridge University Press, Cambridge, UK and New York, NY, USA, <https://doi.org/10.1017/9781009157926.004>, 2022.
- Domingues, C. M., Church, J. A., White, N. J., Gleckler, P. J., Wijffels, S. E., Barker, P. M., and Dunn, J. R.: Improved estimates of upper-ocean warming and multi-decadal sea-level rise, *Nature*, 453, 1090–1093, <https://doi.org/10.1038/nature07080>, 2008.
- 1060 Douville, H., K. Raghavan, J. Renwick, R.P. Allan, P.A. Arias, M. Barlow, R. Cerezo-Mota, A. Cherchi, T.Y. Gan, J. Gergis, D. Jiang, A. Khan, W. Pokam Mba, D. Rosenfeld, J. Tierney, and O. Zolina: Water Cycle Changes. In Climate Change 2021: The Physical Science Basis. Contribution of Working Group I to the Sixth Assessment Report of the Intergovernmental Panel on Climate Change [Masson-Delmotte, V., P. Zhai, A. Pirani, S.L. Connors, C. Péan, S. Berger, N. Caud, Y. Chen, L. Goldfarb, M.I. Gomis, M. Huang, K. Leitzell, E. Lonnoy, J.B.R. Matthews, T.K. Maycock, T. Waterfield, O. Yelekçi, R. Yu, and B.
1065 Zhou (eds.)]. Cambridge University Press, Cambridge, United Kingdom and New York, NY, USA, pp. 1055–1210, <https://doi.org/10.1017/9781009157896.010>, 2021.
- Droste, E. S., Adcock, K. E., Ashfold, M. J., Chou, C., Fleming, Z., Fraser, P. J., Gooch, L. J., Hind, A. J., Langenfelds, R. L., Leedham Elvidge, E. C., Mohd Hanif, N., O'Doherty, S., Oram, D. E., Ou-Yang, C.-F., Panagi, M., Reeves, C. E., Sturges, W. T., and Laube, J. C.: Trends and emissions of six perfluorocarbons in the Northern Hemisphere and Southern Hemisphere,
1070 *Atmos. Chem. Phys.*, 20, 4787–4807, <https://doi.org/10.5194/acp-20-4787-2020>, 2020.

- Dunn, R. J. H., Alexander, L. V., Donat, M. G., Zhang, X., Bador, M., Herold, N., Lippmann, T., Allan, R., Aguilar, E., Barry, A. A., Brunet, M., Caesar, J., Chagnaud, G., Cheng, V., Cinco, T., Durre, I., Guzman, R., Htay, T. M., Wan Ibadullah, W. M., Bin Ibrahim, M. K. I., Khoshkam, M., Kruger, A., Kubota, H., Leng, T. W., Lim, G., Li-Sha, L., Marengo, J., Mbatha, S., McGree, S., Menne, M., Milagros Skansi, M., Ngwenya, S., Nkrumah, F., Oonariya, C., Pabon-Caicedo, J. D., Panthou, G.,
1075 Pham, C., Rahimzadeh, F., Ramos, A., Salgado, E., Salinger, J., Sané, Y., Sopaheluwakan, A., Srivastava, A., Sun, Y., Timbal, B., Trachow, N., Trewin, B., Schrier, G., Vazquez-Aguirre, J., Vasquez, R., Villarroel, C., Vincent, L., Vischel, T., Vose, R., and Bin Hj Yussof, M. N.: Development of an updated global land in situ-based data set of temperature and precipitation extremes: HadEX3, *J. Geophys. Res.-Atmos.*, 125, e2019JD032263, <https://doi.org/10.1029/2019JD032263>, 2020.
- Dunn, R. J. H., Donat, M. G., and Alexander, L. V.: Comparing extremes indices in recent observational and reanalysis
1080 products, *Front. Clim.*, 4, 98905, <https://doi.org/10.3389/fclim.2022.989505>, 2022.
- Eyring, V., N. P. Gillett, K.M. Achuta Rao, R. Barimalala, M. Barreiro Parrillo, N. Bellouin, C. Cassou, P. J. Durack, Y. Kosaka, S. McGregor, S. Min, O. Morgenstern, and Y. Sun: Human Influence on the Climate System. In *Climate Change 2021: The Physical Science Basis. Contribution of Working Group I to the Sixth Assessment Report of the Intergovernmental Panel on Climate Change*[Masson-Delmotte, V., P. Zhai, A. Pirani, S.L. Connors, C. Péan, S. Berger, N. Caud, Y. Chen, L.
1085 Goldfarb, M.I. Gomis, M. Huang, K. Leitzell, E. Lonnoy, J.B.R. Matthews, T.K. Maycock, T. Waterfield, O. Yelekçi, R. Yu, and B. Zhou (eds.)]. Cambridge University Press, Cambridge, United Kingdom and New York, NY, USA, pp. 423–552, <http://doi:10.1017/9781009157896.005>, 2021.
- Forster, P. M., Forster, H. I., Evans, M. J., Gidden, M. J., Jones, C. D., Keller, C. A., Lamboll, R. D., Le Quéré, C., Rogelj, J., Rosen, D., Schleussner, C. F., Richardson, T. B., Smith, C. J. and Turnock, S. T.: Current and future global climate impacts
1090 resulting from COVID-19, *Nature Clim. Chang.*, 10, 913–919, <https://doi.org/10.1038/s41558-020-0883-0>, 2020.
- Forster, P., T. Storelvmo, K. Armour, W. Collins, J.-L. Dufresne, D. Frame, D.J. Lunt, T. Mauritsen, M.D. Palmer, M. Watanabe, M. Wild, and H. Zhang, 2021: The Earth’s Energy Budget, Climate Feedbacks, and Climate Sensitivity. In *Climate Change 2021: The Physical Science Basis. Contribution of Working Group I to the Sixth Assessment Report of the Intergovernmental Panel on Climate Change* [Masson-Delmotte, V., P. Zhai, A. Pirani, S.L. Connors, C. Péan, S. Berger, N.
1095 Caud, Y. Chen, L. Goldfarb, M.I. Gomis, M. Huang, K. Leitzell, E. Lonnoy, J.B.R. Matthews, T.K. Maycock, T. Waterfield, O. Yelekçi, R. Yu, and B. Zhou (eds.)]. Cambridge University Press, Cambridge, United Kingdom and New York, NY, USA, pp. 923–1054, <https://doi.org/10.1017/9781009157896.009>, 2021.
- Fox-Kemper, B., Fox-Kemper, B., H. T. Hewitt, C. Xiao, G. Aðalgeirsdóttir, S.S. Drijfhout, T. L. Edwards, N. R. Golledge, M. Hemer, R. E. Kopp, G. Krinner, A. Mix, D. Notz, S. Nowicki, I. S. Nurhati, L. Ruiz, J.-B. Sallée, A. B. A. Slangen, and Y.
1100 Yu: Ocean, Cryosphere and Sea Level Change. In *Climate Change 2021: The Physical Science Basis. Contribution of Working Group I to the Sixth Assessment Report of the Intergovernmental Panel on Climate Change* [Masson-Delmotte, V., P. Zhai,

- A. Pirani, S.L. Connors, C. Péan, S. Berger, N. Caud, Y. Chen, L. Goldfarb, M.I. Gomis, M. Huang, K. Leitzell, E. Lonnoy, J. B. R. Matthews, T. K. Maycock, T. Waterfield, O. Yelekçi, R. Yu, and B. Zhou (eds.]. Cambridge University Press, Cambridge, United Kingdom and New York, NY, USA, pp. 1211–1362, 1105 <https://doi.org/10.1017/9781009157896.011>, 2021.
- Friedlingstein, P., O’Sullivan, M., Jones, M. W., Andrew, R. M., Hauck, J., Olsen, A., Peters, G. P., Peters, W., Pongratz, J., Sitch, S., Le Quéré, C., Canadell, J. G., Ciais, P., Jackson, R. B., Alin, S., Aragão, L. E. O. C., Arneeth, A., Arora, V., Bates, N. R., Becker, M., Benoit-Cattin, A., Bittig, H. C., Bopp, L., Bultan, S., Chandra, N., Chevallier, F., Chini, L. P., Evans, W., Florentie, L., Forster, P. M., Gasser, T., Gehlen, M., Gilfillan, D., Gkritzalis, T., Gregor, L., Gruber, N., Harris, I., Hartung, 1110 K., Haverd, V., Houghton, R. A., Ilyina, T., Jain, A. K., Joetzer, E., Kadono, K., Kato, E., Kitidis, V., Korsbakken, J. I., Landschützer, P., Lefèvre, N., Lenton, A., Lienert, S., Liu, Z., Lombardozzi, D., Marland, G., Metzl, N., Munro, D. R., Nabel, J. E. M. S., Nakaoka, S.-I., Niwa, Y., O’Brien, K., Ono, T., Palmer, P. I., Pierrot, D., Poulter, B., Resplandy, L., Robertson, E., Rödenbeck, C., Schwinger, J., Séférian, R., Skjelvan, I., Smith, A. J. P., Sutton, A. J., Tanhua, T., Tans, P. P., Tian, H., Tilbrook, B., van der Werf, G., Vuichard, N., Walker, A. P., Wanninkhof, R., Watson, A. J., Willis, D., Wiltshire, A. J., Yuan, 1115 W., Yue, X., and Zaehle, S.: Global carbon budget 2020, *Earth Syst. Sci. Data*, 12, 3269–3340, <https://doi.org/10.5194/essd-12-3269-2020>, 2020.
- Friedlingstein, P., O’Sullivan, M., Jones, M. W., Andrew, R. M., Gregor, L., Hauck, J., Le Quéré, C., Luijkx, I. T., Olsen, A., Peters, G. P., Peters, W., Pongratz, J., Schwingshackl, C., Sitch, S., Canadell, J. G., Ciais, P., Jackson, R. B., Alin, S. R., Alkama, R., Arneeth, A., Arora, V. K., Bates, N. R., Becker, M., Bellouin, N., Bittig, H. C., Bopp, L., Chevallier, F., Chini, L. 1120 P., Cronin, M., Evans, W., Falk, S., Feely, R. A., Gasser, T., Gehlen, M., Gkritzalis, T., Gloege, L., Grassi, G., Gruber, N., Gürses, Ö., Harris, I., Hefner, M., Houghton, R. A., Hurtt, G. C., Iida, Y., Ilyina, T., Jain, A. K., Jersild, A., Kadono, K., Kato, E., Kennedy, D., Klein Goldewijk, K., Knauer, J., Korsbakken, J. I., Landschützer, P., Lefèvre, N., Lindsay, K., Liu, J., Liu, Z., Marland, G., Mayot, N., McGrath, M. J., Metzl, N., Monacci, N. M., Munro, D. R., Nakaoka, S.-I., Niwa, Y., O’Brien, K., Ono, T., Palmer, P. I., Pan, N., Pierrot, D., Pockock, K., Poulter, B., Resplandy, L., Robertson, E., Rödenbeck, C., Rodriguez, 1125 C., Rosan, T. M., Schwinger, J., Séférian, R., Shutler, J. D., Skjelvan, I., Steinhoff, T., Sun, Q., Sutton, A. J., Sweeney, C., Takao, S., Tanhua, T., Tans, P. P., Tian, X., Tian, H., Tilbrook, B., Tsujino, H., Tubiello, F., van der Werf, G. R., Walker, A. P., Wanninkhof, R., Whitehead, C., Willstrand Wranne, A., et al.: Global Carbon Budget 2022, *Earth Syst. Sci. Data*, 14, 4811–4900, <https://doi.org/10.5194/essd-14-4811-2022>, 2022a.
- Friedlingstein, P., O’Sullivan, M., Jones, M. W., Andrew, R. M., Gregor, L., Hauck, L., Le Quéré, C., Luijkx, I. T., Olsen, A., 1130 Peters, G. P., Peters, W., Pongratz, J., Schwingshackl, C., Sitch, S., Canadell, J. G., Ciais, P., Jackson, R. B., Alin, S., Alkama, R., Arneeth, A., Arora, V. K., Bates, N. R., Becker, M., Bellouin, N., Bittig, H. C., Bopp, L., Chevallier, F., Chini, L. P., Cronin, M., Evans, W., Falk, S., Feely, R. A., Gasser, T., Gehlen, M., Gkritzalis, T., Gloege, L., Grassi, G., Gruber, N., Gürses, Ö., Harris, I., Hefner, M., Houghton, R. A., Hurtt, G. C., Iida, Y., Ilyina, T., Jain, A. T., Jersild, A., Kadono, K., Kato, E., Kennedy,

- D., Klein Goldewijk, K., Knauer, J., Korsbakken, J. I., Landschützer, P., Lefèvre, N., Lindsay, Keith., Liu, J., Marland, G.,
1135 Mayot, N., McGrath, M. J., Metzl, N., Monacci, N. M., Munro, D. R., Nakaoka, S.-I., Niwa, Y., O'Brien, K., Ono, T., Palmer,
P. I., Pan, N., Pierrot, D., Pockock, K., Poulter, B., Resplandy, L., Robertson, E., Rödenbeck, C., Rodriguez, C., Rosan, T. M.,
Schwinger, J., Séférian, R., Shutler, J. D., Skjelvan, I., Steinhoff, T., Sun, Q., Sutton, A. J., Sweeney, C., Takao, S., Tanhua,
T., Tans, P. P., Tian, X., Tian, H., Tilbrook, B., Tsujino, H., Tubiello, F., van der Werf, G. R., Walker, A. P., Wanninkhof, R.,
Whitehead, C., Wranne, A., Wright, R. M., Yuan, W., Yue, C., Yue, X., Zaehle, S., Zeng, J., Zheng, B. and Zhu, L.:
1140 Supplemental data of the Global Carbon Budget 2022, ICOS-ERIC Carbon Portal [data set], <https://doi.org/10.18160/GCP-2022>, 2022b.
- Gasser, T., Crepin, L., Quilcaille, Y., Houghton, R. A., Ciais, P., and Obersteiner, M.: Historical CO₂ emissions from land use
and land cover change and their uncertainty, *Biogeosciences*, 17, 4075–4101, <https://doi.org/10.5194/bg-17-4075-2020>, 2020.
- 1145 Gillett, N. P., Shiogama, H., Funke, B., Hegerl, G., Knutti, R., Matthes, K., Santer, B. D., Stone, D., and Tebaldi, C.: The
Detection and Attribution Model Intercomparison Project (DAMIP v1.0) contribution to CMIP6, *Geosci. Model. Dev.*, 9,
3685–3697, <https://doi.org/10.5194/gmd-9-3685-2016>, 2016.
- Gillett, N.P., Kirchmeier-Young, M., Ribes, A., Shiogama, H., Hegerl, G.C., Knutti, R., Gastineau, G., John, J.G., Li, L.,
Nazarenko, L., Rosenbloom, N., Seland, Ø., Wu, T., Yukimoto, S., and Ziehn, T.: Constraining human contributions to
1150 observed warming since the pre-industrial period, *Nat. Clim. Chang.*, 11, 207–212, <https://doi.org/10.1038/s41558-020-00965-9>, 2021.
- Gleckler, P. J., Durack, P. J., Stouffer, R. J., Johnson, G. C., and Forest, C. E.: Industrial-era global ocean heat uptake doubles
in recent decades, *Nat. Clim. Chang.*, 6, 394–398, <https://doi.org/10.1038/nclimate2915>, 2016.
- Good, S. A., Martin, M. J., and Rayner, N. A.: EN4: Quality controlled ocean temperature and salinity profiles and monthly
1155 objective analyses with uncertainty estimates, THE EN4 DATA SET, *J. Geophys. Res.-Oceans*, 118, 6704–6716,
<https://doi.org/10.1002/2013JC009067>, 2013.
- Grassi, G., Schwingshackl, C., Gasser, T., Houghton, R. A., Sitch, S., Canadell, J. G., Cescatti, A., Ciais, P., Federici, S.,
Friedlingstein, P., Kurz, W. A., Sanz Sanchez, M. J., Abad Viñas, R., Alkama, R., Bultan, S., Ceccherini, G., Falk, S., Kato,
E., Kennedy, D., Knauer, J., Korosuo, A., Melo, J., McGrath, M. J., Nabel, J. E. M. S., Poulter, B., Romanovskaya, A. A.,
1160 Rossi, S., Tian, H., Walker, A. P., Yuan, W., Yue, X., and Pongratz, J.: Harmonising the land-use flux estimates of global
models and national inventories for 2000–2020, *Earth Syst. Sci. Data*, 15, 1093–1114, <https://doi.org/10.5194/essd-15-1093-2023>, 2023.
- Guevara, M., Petetin, H., Jorba, O., Denier van der Gon, H., Kuenen, J., Super, I., Granier, C., Doumbia, T., Ciais, P., Liu, Z.,
Lamboll, R. D., Schindlbacher, S., Matthews, B., and Pérez García-Pando, C.: Towards near-real time air pollutant and

- 1165 greenhouse gas emissions: lessons learned from multiple estimates during the COVID-19 Pandemic, *EGUsphere* [preprint],
2023, 1–36, <https://doi.org/10.5194/egusphere-2023-186>, 2023.
- Gulev, S. K., P. W. Thorne, J. Ahn, F. J. Dentener, C. M. Domingues, S. Gerland, D. Gong, D. S. Kaufman, H. C. Nnamchi,
J. Quaas, J.A. Rivera, S. Sathyendranath, S.L. Smith, B. Trewin, K. von Schuckmann, and R. S. Vose: Changing State of the
Climate System. In *Climate Change 2021: The Physical Science Basis. Contribution of Working Group I to the Sixth*
1170 *Assessment Report of the Intergovernmental Panel on Climate Change*[Masson-Delmotte, V., P. Zhai, A. Pirani, S.L. Connors,
C. Péan, S. Berger, N. Caud, Y. Chen, L. Goldfarb, M.I. Gomis, M. Huang, K. Leitzell, E. Lonnoy, J.B.R. Matthews, T.K.
Maycock, T. Waterfield, O. Yelekçi, R. Yu, and B. Zhou (eds.)]. Cambridge University Press, Cambridge, United Kingdom
and New York, NY, USA, pp. 287–422, <https://doi.org/10.1017/9781009157896.004>, 2021.
- Gutiérrez, J. M., R. G. Jones, G. T. Narisma, L. M. Alves, M. Amjad, I. V. Gorodetskaya, M. Grose, N. A. B. Klutse, S.
1175 Krakovska, J. Li, D. Martínez-Castro, L. O. Mearns, S. H. Mernild, T. Ngo-Duc, B. van den Hurk, and J.-H. Yoon: Atlas. In
Climate Change 2021: The Physical Science Basis. Contribution of Working Group I to the Sixth Assessment Report of the
Intergovernmental Panel on Climate Change [Masson-Delmotte, V., P. Zhai, A. Pirani, S.L. Connors, C. Péan, S. Berger, N.
Caud, Y. Chen, L. Goldfarb, M.I. Gomis, M. Huang, K. Leitzell, E. Lonnoy, J.B.R. Matthews, T.K. Maycock, T. Waterfield,
O. Yelekçi, R. Yu, and B. Zhou (eds.)]. Cambridge University Press, Cambridge, United Kingdom and New York, NY, USA,
1180 pp. 1927–2058, <https://doi.org/10.1017/9781009157896.021>, 2021. Note: The companion Interactive Atlas is
available at <http://interactive-atlas.ipcc.ch>
- Gütschow, J., Jeffery, M. L., Gieseke, R., Gebel, R., Stevens, D., Krapp, M., and Rocha, M.: The PRIMAP-hist national
historical emissions time series, *Earth Syst. Sci. Data*, 8, 571–603, <https://doi.org/10.5194/essd-8-571-2016>, 2016.
- Gütschow, J., and Pflüger, M.: The PRIMAP-hist national historical emissions time series (1750-2021) v2.4.1 (2.4.1), Zenodo
1185 [data set], <https://doi.org/10.5281/zenodo.7585420>, 2023.
- Hakuba, M. Z., Frederikse, T., and Landerer, F. W.: Earth's energy imbalance from the ocean perspective (2005–2019),
Geophys Res Lett, 48, e2021GL093624, <https://doi.org/10.1029/2021GL093624>, 2021.
- Hall, B. D., Crotwell, A. M., Kitzis, D. R., Mefford, T., Miller, B. R., Schibig, M. F., and Tans, P. P.: Revision of the World
Meteorological Organization Global Atmosphere Watch (WMO/GAW) CO₂ calibration scale, *Atmos. Meas. Tech.*, 14, 3015–
1190 3032, <https://doi.org/10.5194/amt-14-3015-2021>, 2021.
- Hansis, E., Davis, S. J., and Pongratz, J.: Relevance of methodological choices for accounting of land use change carbon fluxes,
Global Biogeochem. Cy., 29, 1230–1246, <https://doi.org/10.1002/2014GB004997>, 2015.
- Haustein, K., Allen, M. R., Forster, P. M., Otto, F. E. L., Mitchell, D. M., Matthews, H. D., and Frame, D. J.: A real-time
Global Warming Index, *Sci Rep*, 7, 15417, <https://doi.org/10.1038/s41598-017-14828-5>, 2017.

- 1195 Hersbach, H., Bell, B., Berrisford, P., Hirahara, S., Horányi, A., Muñoz-Sabater, J., Nicolas, J., Peubey, C., Radu, R., Schepers, D., Simmons, A., Soci, C., Abdalla, S., Abellan, X., Balsamo, G., Bechtold, P., Biavati, G., Bidlot, J., Bonavita, M., De Chiara, G., Dahlgren, P., Dee, D., Diamantakis, M., Dragani, R., Flemming, J., Forbes, R., Fuentes, M., Geer, A., Haimberger, L., Healy, S., Hogan, R. J., Hólm, E., Janisková, M., Keeley, S., Laloyaux, P., Lopez, P., Lupu, C., Radnoti, G., de Rosnay, P., Rozum, I., Vamborg, F., Villaume, S., and Thépaut, J.-N.: The ERA5 global reanalysis, *Q. J. R. Meteorol. Soc.*, 146, 1999–
- 1200 2049, <https://doi.org/10.1002/qj.3803>, 2020.
- Hodnebrog, Ø., Aamaas, B., Fuglestedt, J. S., Marston, G., Myhre, G., Nielsen, C. J., Sandstad, M., Shine, K. P., and Wallington, T. J.: Updated Global Warming Potentials and Radiative Efficiencies of Halocarbons and Other Weak Atmospheric Absorbers, *Rev. Geophys.*, 58, e2019RG000691, <https://doi.org/10.1029/2019RG000691>, 2020.
- Hoesly, R. M., Smith, S. J., Feng, L., Klimont, Z., Janssens-Maenhout, G., Pitkanen, T., Seibert, J. J., Vu, L., Andres, R. J.,
- 1205 Bolt, R. M., Bond, T. C., Dawidowski, L., Kholod, N., Kurokawa, J.-I., Li, M., Liu, L., Lu, Z., Moura, M. C. P., O'Rourke, P. R., and Zhang, Q.: Historical (1750–2014) anthropogenic emissions of reactive gases and aerosols from the Community Emissions Data System (CEDS), *Geosci. Model. Dev.*, 11, 369–408, <https://doi.org/10.5194/gmd-11-369-2018>, 2018.
- Houghton, R. A., and Nassikas, A. A.: Global and regional fluxes of carbon from land use and land cover change 1850–2015, *Global Biogeochem. Cy.*, 31, 456–472, <https://doi.org/10.1002/2016GB005546>, 2017.
- 1210 IPCC: Climate Change 2013: The Physical Science Basis. Contribution of Working Group I to the Fifth Assessment Report of the Intergovernmental Panel on Climate Change [Stocker, T.F., D. Qin, G.-K. Plattner, M. Tignor, S.K. Allen, J. Boschung, A. Nauels, Y. Xia, V. Bex and P.M. Midgley (eds.)]. Cambridge University Press, Cambridge, United Kingdom and New York, NY, USA, 1535 pp, <https://doi:10.1017/CBO9781107415324>, 2013.
- IPCC: Summary for Policymakers. In: Global Warming of 1.5°C. An IPCC Special Report on the impacts of global warming
- 1215 of 1.5°C above pre-industrial levels and related global greenhouse gas emission pathways, in the context of strengthening the global response to the threat of climate change, sustainable development, and efforts to eradicate poverty [Masson-Delmotte, V., P. Zhai, H.-O. Pörtner, D. Roberts, J. Skea, P.R. Shukla, A. Pirani, W. Moufouma-Okia, C. Péan, R. Pidcock, S. Connors, J.B.R. Matthews, Y. Chen, X. Zhou, M.I. Gomis, E. Lonnoy, T. Maycock, M. Tignor, and T. Waterfield (eds.)]. Cambridge University Press, Cambridge, UK and New York, NY, USA, pp. 3-24, <https://doi.org/10.1017/9781009157940.001>,
- 1220 2018.
- IPCC: Climate Change 2021: The Physical Science Basis. Contribution of Working Group I to the Sixth Assessment Report of the Intergovernmental Panel on Climate Change, Cambridge University Press, Cambridge, United Kingdom and New York, NY, USA, <https://doi.org/10.1017/9781009157896>, 2021a.
- IPCC: Summary for Policymakers, in: Climate Change 2021: The Physical Science Basis. Contribution of Working Group I
- 1225 to the Sixth Assessment Report of the Intergovernmental Panel on Climate Change, edited by: Masson-Delmotte, V., Zhai, P.,

- Pirani, A., Connors, S. L., Péan, C., Berger, S., Caud, N., Chen, Y., Goldfarb, L., Gomis, M. I., Huang, M., Leitzell, K., Lonnoy, E., Matthews, J. B. R., Maycock, T. K., Waterfield, T., Yelekçi, O., Yu, R., and Zhou, B., Cambridge University Press, Cambridge, United Kingdom and New York, NY, USA, pp.3–32 <https://doi.org/10.1017/9781009157896.001>, 2021b.
- 1230 IPCC: Annex III: Tables of historical and projected well-mixed greenhouse gas mixing ratios and effective radiative forcing of all climate forcings [Dentener F.J., B. Hall, C. Smith (eds.)]. In *Climate Change 2021: The Physical Science Basis. Contribution of Working Group I to the Sixth Assessment Report of the Intergovernmental Panel on Climate Change* [Masson-Delmotte, V., P. Zhai, A. Pirani, S.L. Connors, C. Péan, S. Berger, N. Caud, Y. Chen, L. Goldfarb, M.I. Gomis, M. Huang, K. Leitzell, E. Lonnoy, J.B.R. Matthews, T.K. Maycock, T. Waterfield, O. Yelekçi, R. Yu, and B. Zhou (eds.)]. Cambridge University Press, Cambridge, United Kingdom and New York, NY, USA, pp. 2139–2152, <https://doi.org/10.1017/9781009157896.017>, 2021c.
- 1235 IPCC: *Climate Change 2022: Impacts, Adaptation, and Vulnerability. Contribution of Working Group II to the Sixth Assessment Report of the Intergovernmental Panel on Climate Change* [H.-O. Pörtner, D.C. Roberts, M. Tignor, E.S. Poloczanska, K. Mintenbeck, A. Alegría, M. Craig, S. Langsdorf, S. Lösschke, V. Möller, A. Okem, B. Rama (eds.)]. Cambridge University Press. Cambridge University Press, Cambridge, UK and New York, NY, USA, 3056 pp., <https://doi:10.1017/9781009325844>, 2022.
- 1240 Ishii, M., Fukuda, Y., Hirahara, S., Yasui, S., Suzuki, T., and Sato, K.: Accuracy of Global Upper Ocean Heat Content Estimation Expected from Present Observational Data Sets, *SOLA*, 13, 163–167, <https://doi.org/10.2151/sola.2017-030>, 2017.
- 1245 Iturbide, M., Fernández, J., Gutiérrez, J. M., Pirani, A., Huard, D., Al Khourdajie, A., Baño-Medina, J., Bedia, J., Casanueva, A., Cimadevilla, E., Cofiño, A. S., De Felice, M., Diez-Sierra, J., García-Díez, M., Goldie, J., Herrera, D. A., Herrera, S., Manzanas, R., Milovac, J., Radhakrishnan, A., San-Martín, D., Spinuso, A., Thyng, K. M., Trenham, C., and Yelekçi, Ö.: Implementation of FAIR principles in the IPCC: the WGI AR6 Atlas repository, *Sci Data*, 9, 629, <https://doi.org/10.1038/s41597-022-01739-y>, 2022.
- 1250 Jenkins, S., Smith, C., Allen, M., and Grainger, R.: Tonga eruption increases chance of temporary surface temperature anomaly above 1.5 °C, *Nature Clim. Chang.*, 13, 127–129, <https://doi.org/10.1038/s41558-022-01568-2>, 2023.
- Kadow, C., Hall, D. M., and Ulbrich, U.: Artificial intelligence reconstructs missing climate information, *Nat. Geosci.*, 13, 408–413, <https://doi.org/10.1038/s41561-020-0582-5>, 2020.
- 1255 Kirchengast, G., Gorfer, M., Mayer, M., Steiner, A. K., and Haimberger, L.: GCOS EHI 1960-2020 Atmospheric Heat Content, <https://doi.org/10.26050/WDCC/GCOS EHI 1960-2020 AHC>, 2022.

- Kramer, R. J., He, H., Soden, B. J., Oreopoulos, L., Myhre, G., Forster, P. M., and Smith, C. J., Observational evidence of increasing global radiative forcing, *Geophys. Res. Lett.*, 48, e2020GL091585, <https://doi.org/10.1029/2020GL091585>, 2021.
- Lamboll, R. D. and Rogelj, J.: Code for estimation of remaining carbon budget in IPCC AR6 WGI, Zenodo [code], 260 <https://doi.org/10.5281/zenodo.6373365>, 2022.
- Lan, X., Tans, P. and Thoning, K.W.: Trends in globally-averaged CO₂ determined from NOAA Global Monitoring Laboratory measurements, Version 2023-04, <https://doi.org/10.15138/9N0H-ZH07>, 2023a.
- Lan, X., Thoning, K. W., and Dlugokencky, E.J.: Trends in globally-averaged CH₄ N₂O, and SF₆ determined from NOAA Global Monitoring Laboratory measurements, Version 2023-04, <https://doi.org/10.15138/P8XG-AA10>, 2023b.
- 265 Laube, J., Newland, M., Hogan, C., Brenninkmeijer, A.M., Fraser, P.J., Martinerie, P., Oram, D.E., Reeves, C.E., Röckmann, T., Schwander, J., Witrant, E., Sturges, W.T.: Newly detected ozone-depleting substances in the atmosphere. *Nature Geosci.*, 7, 266–269, <https://doi.org/10.1038/ngeo2109>, 2014.
- Lee, J.-Y., J. Marotzke, G. Bala, L. Cao, S. Corti, J.P. Dunne, F. Engelbrecht, E. Fischer, J.C. Fyfe, C. Jones, A. Maycock, J. Mutemi, O. Ndiaye, S. Panickal, and T. Zhou: Future Global Climate: Scenario-Based Projections and Near-Term Information. 270 In *Climate Change 2021: The Physical Science Basis. Contribution of Working Group I to the Sixth Assessment Report of the Intergovernmental Panel on Climate Change*[Masson-Delmotte, V., P. Zhai, A. Pirani, S.L. Connors, C. Péan, S. Berger, N. Caud, Y. Chen, L. Goldfarb, M.I. Gomis, M. Huang, K. Leitzell, E. Lonnoy, J.B.R. Matthews, T.K. Maycock, T. Waterfield, O. Yelekçi, R. Yu, and B. Zhou (eds.)]. Cambridge University Press, Cambridge, United Kingdom and New York, NY, USA, pp. 553–672, <https://doi.org/10.1017/9781009157896.006>, 2021.
- 275 Lee, H., K. Calvin, D. Dasgupta, G. Krinner, A. Mukherji, P. Thorne, C. Trisos, J. Romero, P. Aldunce, K. Barrett, G. Blanco, W.W.L. Cheung, S.L. Connors, F. Denton, A. Diongue-Niang, D. Dodman, M. Garschagen, O. Geden, B. Hayward, C. Jones, F. Jotzo, T. Krug, R. Lasco, J.-Y. Lee, V. Masson-Delmotte, M. Meinshausen, K. Mintenbeck, A. Mokssit, F.E.L. Otto, M. Pathak, A. Pirani, E. Poloczanska, H.-O. Pörtner, A. Revi, D.C. Roberts, J. Roy, A.C. Ruane, J. Skea, P.R. Shukla, R. Slade, A. Slangen, Y. Sokona, A.A. Sörensson, M. Tignor, D. van Vuuren, Y.-M. Wei, H. Winkler, P. Zhai, and Z. Zommers: 280 Synthesis Report of the IPCC Sixth Assessment Report (AR6): Summary for Policymakers. Intergovernmental Panel on Climate Change [accepted], available at <https://www.ipcc.ch/report/ar6/syr/>, 2023.
- Lenssen, N. J. L., Schmidt, G. A., Hansen, J. E., Menne, M. J., Persin, A., Ruedy, R., and Zyss, D.: Improvements in the GISTEMP Uncertainty Model, *J. Geophys. Res.-Atmos.*, 124, 6307–6326, <https://doi.org/10.1029/2018JD029522>, 2019.

- 1285 Levitus, S., Antonov, J. I., Boyer, T. P., Baranova, O. K., Garcia, H. E., Locarnini, R. A., Mishonov, A. V., Reagan, J. R., Seidov, D., Yarosh, E. S., and Zweng, M. M.: World ocean heat content and thermosteric sea level change (0–2000 m), 1955–2010, *Geophys. Res. Lett.*, 39, <https://doi.org/10.1029/2012GL051106>, 2012.
- Loeb, N. G., Johnson, G. C., Thorsen, T. J., Lyman, J. M., Rose, F. G., Kato, S.: Satellite and ocean data reveal marked increase in Earth’s heating rate. *Geophys. Res. Lett.*, 48, e2021GL093047, <https://doi.org/10.1029/2021GL093047>, 2021.
- 1290 Lonsdale, C. R. and Sun, K.: Nitrogen oxides emissions from selected cities in North America, Europe, and East Asia observed by TROPOMI before and after the COVID-19 pandemic, *EGUsphere* [preprint], 2023, 1–30, <https://doi.org/10.5194/egusphere-2023-346>, 2023.
- van Marle, M. J. E., Kloster, S., Magi, B. I., Marlon, J. R., Daniau, A.-L., Field, R. D., Arneth, A., Forrest, M., Hantson, S., Kehrwald, N. M., Knorr, W., Lasslop, G., Li, F., Mangeon, S., Yue, C., Kaiser, J. W., and van der Werf, G. R.: Historic global biomass burning emissions for CMIP6 (BB4CMIP) based on merging satellite observations with proxies and fire models (1750–2015), *Geosci. Model Dev.*, 10, 3329–3357, <https://doi.org/10.5194/gmd-10-3329-2017>, 2017.
- 1295 McKenna, C. M., Maycock, A. C., Forster, P. M., Smith, C. J., and Tokarska, K. B.: Stringent mitigation substantially reduces risk of unprecedented near-term warming rates, *Nature Climate Change*, 11, 126–131, <https://doi.org/10.1038/s41558-020-00957-9>, 2021.
- 1300 Meinshausen, M., Raper, S. C. B., and Wigley, T. M. L.: Emulating coupled atmosphere-ocean and carbon cycle models with a simpler model, *MAGICC6 – Part 1: Model description and calibration*, *Atmos. Chem. Phys.*, 11, 1417–1456, <https://doi.org/10.5194/acp-11-1417-2011>, 2011.
- Millán, L., Santee, M. L., Lambert, A., Livesey, N. J., Werner, F., Schwartz, M. J., Pumphrey, H. C., Manney, G. L., Wang, Y., Su, H., Wu, L., Read, W. G., and Froidevaux, L.: The Hunga Tonga-Hunga Ha’apai Hydration of the Stratosphere, *Geophys. Res. Lett.*, 49, e2022GL099381, <https://doi.org/10.1029/2022GL099381>, 2022.
- 1305 Minx, J. C., Lamb, W. F., Andrew, R. M., Canadell, J. G., Crippa, M., Döbbeling, N., Forster, P. M., Guizzardi, D., Olivier, J., Peters, G. P., Pongratz, J., Reisinger, A., Rigby, M., Saunois, M., Smith, S. J., Solazzo, E., and Tian, H.: A comprehensive and synthetic dataset for global, regional, and national greenhouse gas emissions by sector 1970–2018 with an extension to 2019, *Earth Syst. Sci. Data*, 13, 5213–5252, <https://doi.org/10.5194/essd-13-5213-2021>, 2021.
- 1310 Montzka, S: The NOAA Annual Greenhouse Gas Index (AGGI), <https://gml.noaa.gov/aggi/aggi.html>, 2022.
- Myhre, G., D. Shindell, F.-M. Bréon, W. Collins, J. Fuglestedt, J. Huang, D. Koch, J.-F. Lamarque, D. Lee, B. Mendoza, T. Nakajima, A. Robock, G. Stephens, T. Takemura and H. Zhang: Anthropogenic and Natural Radiative Forcing. In: *Climate Change 2013: The Physical Science Basis. Contribution of Working Group I to the Fifth Assessment Report of the Intergovernmental Panel on Climate Change*, edited by Stocker, T.F., D. Qin, G.-K. Plattner, M. Tignor, S.K. Allen, J.

- 1315 Boschung, A. Nauels, Y. Xia, V. Bex and P.M. Midgley (eds.]. Cambridge University Press, Cambridge, United Kingdom and New York, NY, USA, <https://doi.org/10.1017/CBO9781107415324.018>, 2013.
- Nisbet, E. G., Manning, M. R., Dlugokencky, E. J., Michel, S. E., Lan, X., Roeckmann, T., Gon, H. A. D. V. D., Palmer, P., Oh, Y., Fisher, R., Lowry, D., France, J. L., and White, J. W. C.: Atmospheric methane: Comparison between methane's record in 2006-2022 and during glacial terminations, Preprints, <https://doi.org/10.22541/essoar.167689502.25042797/v1>, 2023.
- 1320 Nitzbon, J., Krinner, G., Deimling, T. S. von, Werner, M., and Langer, M.: Quantifying the Permafrost Heat Sink in Earth's Climate System, ESS Open Archive [preprint], <https://doi.org/10.1002/essoar.10511600.1>, 2022a.
- Nitzbon, J., Krinner, G., Langer, M.: GCOS EHI 1960-2020 Permafrost Heat Content, World Data Center for Climate (WDCC) at DKRZ, https://doi.org/10.26050/WDCC/GCOS_EHI_1960-2020_PHC, 2022b.
- O'Rourke, Patrick R, Smith, Steven J, Mott, Andrea, Ahsan, Hamza, McDuffie, Erin E, Crippa, Monica, Klimont, Zbigniew,
- 1325 McDonald, Brian, Wang, Shuxiao, Nicholson, Matthew B, Feng, Leyang, & Hoesly, Rachel M.: CEDS v_2021_04_21 Release Emission Data (v_2021_02_05), Zenodo [data set], <https://doi.org/10.5281/zenodo.4741285>, 2021.
- Palmer, M. D. and McNeall, D. J.: Internal variability of Earth's energy budget simulated by CMIP5 climate models, Environ. Res. Lett., 9, 034016, <https://doi.org/10.1088/1748-9326/9/3/034016>, 2014.
- Palmer, M. D., Domingues, C. M., Slangen, A. B. A., and Dias, F. B.: An ensemble approach to quantify global mean sea-
- 1330 level rise over the 20th century from tide gauge reconstructions, Environ. Res. Lett., 16, 044043, <https://doi.org/10.1088/1748-9326/abdae>, 2021.
- Peng, S., Lin, X., Thompson, R. L., Xi, Y., Liu, G., Hauglustaine, D., Lan, X., Poulter, B., Ramonet, M., Saunois, M., Yin, Y., Zhang, Z., Zheng, B., and Ciais, P.: Wetland emission and atmospheric sink changes explain methane growth in 2020, Nature, 612, 477–482, <https://doi.org/10.1038/s41586-022-05447-w>, 2022.
- 1335 Pirani, A., Alegria, A., Khourdajie, A. A., Gunawan, W., Gutiérrez, J. M., Holsman, K., Huard, D., Jukes, M., Kawamiya, M., Klutse, N., Krey, V., Matthews, R., Milward, A., Pascoe, C., Van Der Shrier, G., Spinuso, A., Stockhause, M., and Xiaoshi Xing: The implementation of FAIR data principles in the IPCC AR6 assessment process, <https://doi.org/10.5281/ZENODO.6504469>, 2022.
- Pongratz, J., Schwingshackl, C., Bultan, S., Obermeier, W., Havermann, F., and Guo, S.: Land Use Effects on Climate: Current
- 1340 State, Recent Progress, and Emerging Topics, Curr. Clim. Change Rep., 7, 99–120, <https://doi.org/10.1007/s40641-021-00178-y>, 2021.
- Purkey, S.G. and Johnson, G.C., Warming of Global Abyssal and Deep Southern Ocean Waters between the 1990s and 2000s: Contributions to Global Heat and Sea Level Rise Budgets, J. Climate, 23, 6336–6351, <https://doi.org/10.1175/2010JCLI3682.1>, 2010.

- 1345 Putaud, J.-P., Pisoni, E., Mangold, A., Hueglin, C., Sciare, J., Pikridas, M., Savvides, C., Ondracek, J., Mbengue, S., Wiedensohler, A., Weinhold, K., Merkel, M., Poulain, L., van Pinxteren, D., Herrmann, H., Massling, A., Nordstroem, C., Alastuey, A., Reche, C., Pérez, N., Castillo, S., Sorribas, M., Adame, J. A., Petaja, T., Lehtipalo, K., Niemi, J., Riffault, V., de Brito, J. F., Colette, A., Favez, O., Petit, J.-E., Gros, V., Gini, M. I., Vratolis, S., Eleftheriadis, K., Diapouli, E., Denier van der Gon, H., Yttri, K. E., and Aas, W.: Impact of 2020 COVID-19 lockdowns on particulate air pollution across Europe, EGUsphere [preprint], <https://doi.org/10.5194/egusphere-2023-434>, 2023.
- 1350 Quaas, J., Jia, H., Smith, C., Albright, A. L., Aas, W., Bellouin, N., Boucher, O., Doutriaux-Boucher, M., Forster, P. M., Grosvenor, D., Jenkins, S., Klimont, Z., Loeb, N. G., Ma, X., Naik, V., Paulot, F., Stier, P., Wild, M., Myhre, G., and Schulz, M.: Robust evidence for reversal of the trend in aerosol effective climate forcing, *Atmos. Chem. Phys.*, 22, 12221–12239, <https://doi.org/10.5194/acp-22-12221-2022>, 2022.
- 1355 Raghuraman, S.P., Paynter, D. and Ramaswamy, V.: Anthropogenic forcing and response yield observed positive trend in Earth’s energy imbalance, *Nat. Commun.* 12, 4577, <https://doi.org/10.1038/s41467-021-24544-4>, 2021.
- Randerson, J. T., van der Werf, G. R., Giglio, L., Collatz, G. J., and Kasibhatla, P. S.: Global Fire Emissions Database, Version 4.1 (GFEDv4), ORNL Distributed Active Archive Center [dataset], <https://doi.org/10.3334/ORNLDAAAC/1293>, 2017
- 1360 Riahi, K., Schaeffer, J. Arango, K. Calvin, C. Guivarch, T. Hasegawa, K. Jiang, E. Kriegler, R. Matthews, G.P. Peters, A. Rao, S. Robertson, A.M. Sebbit, J. Steinberger, M. Tavoni, D.P. van Vuuren, 2022: Mitigation pathways compatible with long-term goals. In IPCC, 2022: Climate Change 2022: Mitigation of Climate Change. Contribution of Working Group III to the Sixth Assessment Report of the Intergovernmental Panel on Climate Change [P.R. Shukla, J. Skea, R. Slade, A. Al Khourdajie, R. van Diemen, D. McCollum, M. Pathak, S. Some, P. Vyas, R. Fradera, M. Belkacemi, A. Hasija, G. Lisboa, S. Luz, J. Malley, (eds.)]. Cambridge University Press, Cambridge, UK and New York, NY, USA, <https://doi.org/10.1017/9781009157926.005>, 2022.
- 1365 Ribes, A., Qasmi, S., and Gillett, N. P.: Making climate projections conditional on historical observations, *Sci. Adv.*, 7, eabc0671, <https://doi.org/10.1126/sciadv.abc0671>, 2021.
- Richardson, M., Cowtan, K., and Millar, R. J.: Global temperature definition affects achievement of long-term climate goals, *Environ. Res. Lett.*, 13, 054004, <https://doi.org/10.1088/1748-9326/aab305>, 2018.
- 1370 Rogelj, J., D. Shindell, K. Jiang, S. Fifita, P. Forster, V. Ginzburg, C. Handa, H. Khesghi, S. Kobayashi, E. Kriegler, L. Mundaca, R. Sférian, and M. V. Vilariño: Mitigation Pathways Compatible with 1.5°C in the Context of Sustainable Development. In: Global Warming of 1.5°C. An IPCC Special Report on the impacts of global warming of 1.5°C above pre-industrial levels and related global greenhouse gas emission pathways, in the context of strengthening the global response to the threat of climate change, sustainable development, and efforts to eradicate poverty [Masson-Delmotte, V., P. Zhai, H.-O.
- 1375 Pörtner, D. Roberts, J. Skea, P.R. Shukla, A. Pirani, W. Moufouma-Okia, C. Péan, R. Pidcock, S. Connors, J. B. R. Matthews,

- Y. Chen, X. Zhou, M. I. Gomis, E. Lonnoy, T. Maycock, M. Tignor, and T. Waterfield (eds.]. Cambridge University Press, Cambridge, UK and New York, NY, USA, pp. 93-174, <https://doi.org/10.1017/9781009157940.004>, 2018.
- Rogelj, J., Forster, P. M., Kriegler, E., Smith, C. J., and S  f  rian, R.: Estimating and tracking the remaining carbon budget for stringent climate targets, *Nature*, 571, 335–342, <https://doi.org/10.1038/s41586-019-1368-z>, 2019.
- 1380 Rogelj, J., Rao, S., McCollum, D. L., Pachauri, S., Klimont, Z., Krey, V., and Riahi, K: Air-pollution emission ranges consistent with the representative concentration pathways, *Nature Clim. Chang.*, 4 (6), 446–450, <https://doi.org/10.1038/nclimate2178>, 2014.
- Rohde, R., Muller, R., Jacobsen, R., Perlmutter, S., Rosenfeld, A. et al.: Berkeley Earth Temperature Averaging Process, *Geoinfor. Geostat.: An Overview 1:2.*, <http://dx.doi.org/10.4172/gigs.1000103>, 2013.
- 1385 Schoenenberger, F., Vollmer, M.K., Rigby, M., Hill, M., Fraser, P.J., Krummel, P.B., Langenfelds, R.L., Rhee, T.S., Peter, T., Reimann, S.: First observations, trends, and emissions of HCFC-31 (CH₂ClF) in the global atmosphere, *Geophys. Res. Lett.*, 42, 7817–7824, <https://doi.org/10.1002/2015GL064709>, 2015.
- von Schuckmann, K., Cheng, L., Palmer, M. D., Hansen, J., Tassone, C., Aich, V., Adusumilli, S., Beltrami, H., Boyer, T., Cuesta-Valero, F. J., Desbruy  res, D., Domingues, C., Garc  a-Garc  a, A., Gentine, P., Gilson, J., Gorfer, M., Haimberger, L., 1390 Ishii, M., Johnson, G. C., Killick, R., King, B. A., Kirchengast, G., Kolodziejczyk, N., Lyman, J., Marzeion, B., Mayer, M., Monier, M., Monselesan, D. P., Purkey, S., Roemmich, D., Schweiger, A., Seneviratne, S. I., Shepherd, A., Slater, D. A., Steiner, A. K., Straneo, F., Timmermans, M.-L., and Wjiffels, S. E.: Heat stored in the Earth system: where does the energy go?, *Earth Syst. Sci. Data*, 12, 2013–2041, <https://doi.org/10.5194/essd-12-2013-2020>, 2020.
- von Schuckmann, K., Mini  re, A., Gues, F., Cuesta-Valero, F. J., Kirchengast, G., Adusumilli, S., Straneo, F., Ablain, M., 1395 Allan, R. P., Barker, P. M., Beltrami, H., Blazquez, A., Boyer, T., Cheng, L., Church, J., Desbruy  res, D., Dolman, H., Domingues, C. M., Garc  a-Garc  a, A., Giglio, D., Gilson, J. E., Gorfer, M., Haimberger, L., Hakuba, M. Z., Hendricks, S., Hosoda, S., Johnson, G. C., Killick, R., King, B., Kolodziejczyk, N., Korosov, A., Krinner, G., Kuusela, M., Landerer, F. W., Langer, M., Lavergne, T., Lawrence, I., Li, Y., Lyman, J., Marti, F., Marzeion, B., Mayer, M., MacDougall, A. H., McDougall, T., Monselesan, D. P., Nitzbon, J., Otsaka, I., Peng, J., Purkey, S., Roemmich, D., Sato, K., Sato, K., Savita, A., Schweiger, 1400 A., Shepherd, A., Seneviratne, S. I., Simons, L., Slater, D. A., Slater, T., Steiner, A. K., Suga, T., Szekeley, T., Thiery, W., Timmermans, M.-L., Vanderkelen, I., Wjiffels, S. E., Wu, T., and Zemp, M.: Heat stored in the Earth system 1960–2020: where does the energy go?, *Earth System Science Data*, 15, 1675–1709, <https://doi.org/10.5194/essd-15-1675-2023>, 2023a.
- von Schuckmann, K., Mini  re, A., Gues, F., Cuesta-Valero, F. J., Kirchengast, G., Adusumilli, S., Straneo, F., Ablain, M., 1405 Allan, R. P., Barker, P. M., Beltrami, H., Blazquez, A., Boyer, T., Cheng, L., Church, J., Desbruy  res, D., Dolman, H., Domingues, C. M., Garc  a-Garc  a, A., Giglio, D., Gilson, J. E., Gorfer, M., Haimberger, L., Hakuba, M. Z., Hendricks, S.,

Hosoda, S., Johnson, G. C., Killick, R., King, B., Kolodziejczyk, N., Korosov, A., Krinner, G., Kuusela, M., Landerer, F. W., Langer, M., Lavergne, T., Lawrence, I., Li, Y., Lyman, J., Marti, F., Marzeion, B., Mayer, M., MacDougall, A. H., McDougall, T., Monselesan, D. P., Nitzbon, J., Ootaka, I., Peng, J., Purkey, S., Roemmich, D., Sato, K., Sato, K., Savita, A., Schweiger, A., Shepherd, A., Seneviratne, S. I., Simons, L., Slater, D. A., Slater, T., Steiner, A. K., Suga, T., Szekely, T., Thiery, W., Timmermans, M.-L., Vanderkelen, I., Wjiffels, S. E., Wu, T., and Zemp, M.: GCOS EHI 1960-2020 Earth Heat Inventory Ocean Heat Content (Version 2), https://doi.org/10.26050/WDCC/GCOS_EHI_1960-2020_OHC_v2, 2023b.

Sellitto, P., Podglajen, A., Belhadji, R., Boichu, M., Carboni, E., Cuesta, J., Duchamp, C., Kloss, C., Siddans, R., Bègue, N., Blarel, L., Jegou, F., Khaykin, S., Renard, J.-B., and Legras, B.: The unexpected radiative impact of the Hunga Tonga eruption of 15th January 2022, *Commun Earth Environ*, 3, 288, <https://doi.org/10.1038/s43247-022-00618-z>, 2022.

Seneviratne, S.I., X. Zhang, M. Adnan, W. Badi, C. Dereczynski, A. Di Luca, S. Ghosh, I. Iskandar, J. Kossin, S. Lewis, F. Otto, I. Pinto, M. Satoh, S. M. Vicente-Serrano, M. Wehner, and B. Zhou: Weather and Climate Extreme Events in a Changing Climate. In *Climate Change 2021: The Physical Science Basis. Contribution of Working Group I to the Sixth Assessment Report of the Intergovernmental Panel on Climate Change* [Masson-Delmotte, V., P. Zhai, A. Pirani, S.L. Connors, C. Péan, S. Berger, N. Caud, Y. Chen, L. Goldfarb, M.I. Gomis, M. Huang, K. Leitzell, E. Lonnoy, J.B.R. Matthews, T.K. Maycock, T. Waterfield, O. Yelekçi, R. Yu, and B. Zhou (eds.)]. Cambridge University Press, Cambridge, United Kingdom and New York, NY, USA, pp. 1513–1766, doi:10.1017/9781009157896.013.1513–1766, <https://doi.org/10.1017/9781009157896.013>, 2021.

Sigl, M., Toohey, M., McConnell, J. R., Cole-Dai, J., and Severi, M.: Volcanic stratospheric sulfur injections and aerosol optical depth during the Holocene (past 11\,500 years) from a bipolar ice-core array, *Earth Syst. Sci. Data*, 14, 3167–3196, <https://doi.org/10.5194/essd-14-3167-2022>, 2022.

Simmonds, P. G., Rigby, M., McCulloch, A., O'Doherty, S., Young, D., Mühle, J., Krummel, P. B., Steele, P., Fraser, P. J., Manning, A. J., Weiss, R. F., Salameh, P. K., Harth, C. M., Wang, R. H. J., and Prinn, R. G.: Changing trends and emissions of hydrochlorofluorocarbons (HCFCs) and their hydrofluorocarbon (HFCs) replacements, *Atmos. Chem. Phys.*, 17, 4641–4655, <https://doi.org/10.5194/acp-17-4641-2017>, 2017.

Sippel, S., Zscheischler, J., Heimann, M., Otto, F. E. L., Peters, J., and Mahecha, M. D.: Quantifying changes in climate variability and extremes: Pitfalls and their overcoming, *Geophys. Res. Lett.*, 42, 9990–9998, <https://doi.org/10.1002/2015GL066307>, 2015.

Smith, C., Nicholls, Z. R. J., Armour, K., Collins, W., Forster, P., Meinshausen, M., Palmer, M. D., and Watanabe, M.: The Earth's Energy Budget, Climate Feedbacks, and Climate Sensitivity Supplementary Material, in: *Climate Change 2021: The Physical Science Basis. Contribution of Working Group I to the Sixth Assessment Report of the Intergovernmental Panel on Climate Change*, edited by: Masson-Delmotte, V., Zhai, P., Pirani, A., Connors, S. L., Péan, C., Berger, S., Caud, N., Chen,

- Y., Goldfarb, L., Gomis, M. I., Huang, M., Leitzell, K., Lonnoy, E., Matthews, J. B. R., Maycock, T. K., Waterfield, T., Yelekçi, O., Yu, R., and Zhou, B., 2021.
- 1440 Smith, C., Walsh, T., Forster, P.M., Gillett, N., Hauser, M., Lamb, W., Lamboll, R., Palmer, M., Ribes, A., Schumacher, D., Seneviratne, S., Trewin, B., and von Schuckmann, K.: Indicators of Global Climate Change 2022 (v2023.05.25), Zenodo. <https://doi.org/10.5281/zenodo.7969114>, 2023.
- Smith, S. J., van Aardenne, J., Klimont, Z., Andres, R. J., Volke, A., and Delgado Arias, S.: Anthropogenic sulfur dioxide emissions: 1850–2005, *Atmos. Chem. and Phys.*, 11, 1101–1116, <https://doi.org/10.5194/acp-11-1101-2011>, 2011.
- 1445 Sokhi, R. S., Singh, V., Querol, X., Finardi, S., Targino, A. C., Andrade, M. de F., Pavlovic, R., Garland, R. M., Massagué, J., Kong, S., Baklanov, A., Ren, L., Tarasova, O., Carmichael, G., Peuch, V.-H., Anand, V., Arbilla, G., Badali, K., Beig, G., Belalcazar, L. C., Bolignano, A., Brimblecombe, P., Camacho, P., Casallas, A., Charland, J.-P., Choi, J., Chourdakis, E., Coll, I., Collins, M., Cyrus, J., Silva, C. M. da, Giosa, A. D. D., Leo, A. D., Ferro, C., Gavidia-Calderon, M., Gayen, A., Ginzburg, A., Godefroy, F., Gonzalez, Y. A., Guevara-Luna, M., Haque, S. M., Havenga, H., Herod, D., Hörrak, U., Hussein, T., Ibarra, S., Jaimes, M., Kaasik, M., Khaiwal, R., Kim, J., Kousa, A., Kukkonen, J., Kulmala, M., Kuula, J., Violette, N. L., Lanzani, G., Liu, X., MacDougall, S., Manseau, P. M., Marchegiani, G., McDonald, B., Mishra, S. V., Molina, L. T., Mooibroek, D., 1450 Mor, S., Moussiopoulos, N., Murena, F., Niemi, J. V., Noe, S., Nogueira, T., Norman, M., Pérez-Camaño, J. L., Petäjä, T., Piketh, S., Rathod, A., Reid, K., Retama, A., Rivera, O., Rojas, N. Y., Rojas-Quincho, J. P., José, R. S., Sánchez, O., Seguel, R. J., Sillanpää, S., Su, Y., Tapper, N., Terrazas, A., Timonen, H., Toscano, D., Tsegas, G., Velders, G. J. M., Vlachokostas, C., Schneidmesser, E. von, VPM, R., Yadav, R., Zalakeviciute, R., and Zavala, M.: A global observational analysis to understand changes in air quality during exceptionally low anthropogenic emission conditions, *Environment International*, 157, 106818, <https://doi.org/10.1016/j.envint.2021.106818>, 2021.
- Steiner, A. K., Ladstädter, F., Randel, W. J., Maycock, A. C., Fu, Q., Claud, C., Gleisner, H., Haimberger, L., Ho, S.-P., Keckhut, P., Leblanc, T., Mears, C., Polvani, L. M., Santer, B. D., Schmidt, T., Sofieva, V., Wing, R., and Zou, C.-Z.: Observed 1460 Temperature Changes in the Troposphere and Stratosphere from 1979 to 2018, *J. Climate*, 33, 8165–8194, <https://doi.org/10.1175/JCLI-D-19-0998.1>, 2020.
- Szopa, S., V. Naik, B. Adhikary, P. Artaxo, T. Berntsen, W.D. Collins, S. Fuzzi, L. Gallardo, A. Kiendler-Scharr, Z. Klimont, H. Liao, N. Unger, and P. Zanis: Short-Lived Climate Forcers. In *Climate Change 2021: The Physical Science Basis. Contribution of Working Group I to the Sixth Assessment Report of the Intergovernmental Panel on Climate Change* [Masson-Delmotte, V., P. Zhai, A. Pirani, S.L. Connors, C. Péan, S. Berger, N. Caud, Y. Chen, L. Goldfarb, M.I. Gomis, M. Huang, K. Leitzell, E. Lonnoy, J.B.R. Matthews, T.K. Maycock, T. Waterfield, O. Yelekçi, R. Yu, and B. Zhou (eds.)]. Cambridge University Press, Cambridge, United Kingdom and New York, NY, USA, pp. 817–922, <https://doi:10.1017/9781009157896.008>, 2021.

- Trewin, B.: Assessing Internal Variability of Global Mean Surface Temperature From Observational Data and Implications for Reaching Key Thresholds, *Journal of Geophysical Research: Atmospheres*, 127, e2022JD036747, <https://doi.org/10.1029/2022JD036747>, 2022.
- Van Der Werf, G. R., Randerson, J. T., Giglio, L., Van Leeuwen, T. T., Chen, Y., Rogers, B. M., Mu, M., Van Marle, M. J. E., Morton, D. C., Collatz, G. J., Yokelson, R. J., and Kasibhatla, P. S.: Global fire emissions estimates during 1997–2016, *Earth Syst. Sci. Data*, 9, 697–720, <https://doi.org/10.5194/essd-9-697-2017>, 2017.
- Vanderkelen, I., van Lipzig, N. P. M., Lawrence, D. M., Droppers, B., Golub, M., Gosling, S. N., Janssen, A. B. G., Marcé, R., Schmied, H. M., Perroud, M., Pierson, D., Pokhrel, Y., Satoh, Y., Schewe, J., Seneviratne, S. I., Stepanenko, V. M., Tan, Z., Woolway, R. I., and Thiery, W.: Global Heat Uptake by Inland Waters, *Geophysical Research Letters*, 47, e2020GL087867, <https://doi.org/10.1029/2020GL087867>, 2020.
- Vanderkelen, I. and Thiery, W.: GCOS EHI 1960-2020 Inland Water Heat Content, https://doi.org/10.26050/WDCC/GCOS_EHI_1960-2020_IWHC, 2022.
- Vollmer, M. K., Young, D., Trudinger, C. M., Mühle, J., Henne, S., Rigby, M., Park, S., Li, S., Guillevic, M., Mitrevski, B., Harth, C. M., Miller, B. R., Reimann, S., Yao, B., Steele, L. P., Wyss, S. A., Lunder, C. R., Arduini, J., McCulloch, A., Wu, S., Rhee, T. S., Wang, R. H. J., Salameh, P. K., Hermansen, O., Hill, M., Langenfelds, R. L., Ivy, D., O'Doherty, S., Krummel, P. B., Maione, M., Etheridge, D. M., Zhou, L., Fraser, P. J., Prinn, R. G., Weiss, R. F., and Simmonds, P. G.: Atmospheric histories and emissions of chlorofluorocarbons CFC-13 (CClF₃), Σ CFC-114 (C₂Cl₂F₄), and CFC-115 (C₂ClF₅), *Atmos. Chem. Phys.*, 18, 979–1002, <https://doi.org/10.5194/acp-18-979-2018>, 2018.
- Western, L. M., Vollmer, M. K., Krummel, P. B., Adcock, K. E., Fraser, P. J., Harth, C. M., Langenfelds, R. L., Montzka, S. A., Mühle, J., O'Doherty, S., Oram, D. E., Reimann, S., Rigby, M., Vimont, I., Weiss, R. F., Young, D., and Laube, J. C.: Global increase of ozone-depleting chlorofluorocarbons from 2010 to 2020, *Nat. Geosci.*, 16, 309–313, <https://doi.org/10.1038/s41561-023-01147-w>, 2023.
- Wild, M., Gilgen, H., Roesch, A., Ohmura, A., Long, C. N., Dutton, E. G., Forgan, B., Kallis, A., Russak, V., and Tsvetkov, A.: From Dimming to Brightening: Decadal Changes in Solar Radiation at Earth's Surface, *Science*, 308, 847–850, <https://doi.org/10.1126/science.1103215>, 2005.
- Zhang, Z., Poulter, B., Feldman, A.F., Ying, Q., Ciais, P., Peng, S. and Xin, L.: Recent intensification of wetland methane feedback, *Nat. Clim. Chang.* 13, 430–433, <https://doi.org/10.1038/s41558-023-01629-0>, 2023.